The stabilisation and scanning of a magnetic field by nuclear magnetic resonance

Author:
Marsden, Kenneth Hulme

Publication Date:
1959

DOI:
https://doi.org/10.26190/unsworks/7556

C E R T I F I C A T E

School of Applied Physics

February, 1959

The Professor of Applied Physics
School of Applied Physics,
University of New South Wales,
Kensington.

The following thesis is respectfully submitted for examination as partial requirement for the award of Master of Science Degree.

I hereby certify that work embodied in this thesis has not been submitted to any other University of Institution for the award of a Higher Degree.

K.H.Marsden

THE STABILISATION AND SCANNING OF A MAGNETIC FIELD BY NUCLEAR MAGNETIC RESONANCE

THESIS

for the degree of

MASTER OF SCIENCE

in the

Faculty of Science,

The University of New South Wales

Submitted by

K.H.Marsden

PREFACE

The School of Applied Physics, University of New South Wales possesses a large 18 KW electromagnet, which is used as a research tool in nuclear magnetic resonance, mass spectrometry and similar topics. In the former case, and particularly in conjunction with spin-echo techniques, it is necessary that the magnetic field should be kept constant in time or should be varied slowly at a given rate over a given range.

It is the object of this thesis to describe how this has been accomplished.

In Section I, a survey is given of the fluctuations likely to be encountered in field of a large electromagnet and of stabilisation methods that have been employed. This section also includes a resumé of the terminology and principles of servomechanism theory employed in later sections.

The frequency response characteristics of the electromagnet and of the d.c. generator used to energise the magnet are described in Section II, together with an analysis of the fluctuations that exist in field of the magnet.

In Section III are described the methods by which the rapid fluctuations are reduced to negligible properties and the magnet field is "smoothed" sufficiently to enable a nuclear magnetic resonance field discriminator to operate and provide a correction for slow drift of the magnetic field.

The theory and principles of operation of two types of

nuclear magnetic resonance absorption signal detectors are discussed in Section IV, while in Section V the application of one of these to act as a magnetic field discriminator is described.

The slow drift feedback loop is discussed in Section VI and a specification of the performance of the whole stabilising system is given. The thesis concludes with some comments on the limitations of the system, and suggests possible methods of further improving the degree of stability of the magnetic field.

CONTENTS

List of Symbols

(Only those symbols having special significance in the text are included.)

Symbol	Defined on page	Meaning
R	5	Reference input to a feedback control system
C	5	Controlled output of a feedback control system
G	5	Transfer function of an element in the foreward loop of a feedback control system
H	5	Transfer function of the feedback loop of a feedback control system
τ	6	Time constant.
U	10	Unwanted disturbance injected into the system.
C_u	10	Response of the controlled output to the disturbance.
G_g	18	Transfer function of the generator
τ_g	18	Time constant of the generator.
G_i	20	Transfer function for the magnet current.
τ_c	20	Time constant associated with the main excitation coils.
τ_e	20	Time constant associated with the eddy currents in the magnet core.
G_m	22	Transfer function the magnet field.
τ_m	22	Time constant for the magnet field.
H_o	35	Static value of the magnetic field.
H	35	Value of the magnet field at resonance.
$2H_1$	35	Amplitude of the r.f. field applied at right-angles to H_o
ω_o	35	Frequency of the applied r.f. field.
γ	35	Gyro-magnetic ratio for the nuclei of the sample.
χ	35	Nuclear susceptibility.

Symbol	Defined on page	Meaning
χ', χ''	35	Real and imaginary parts respectively of the nuclear susceptibility
ζ	35	Filling factor of sample volume within the coil.
χ_0	37	Static (macroscopic) susceptibility of the sample.
T_2	37	Spin-spin or transverse relaxation time.
ΔH	37	*Linewidth of N.M.R. absorption signal measured at half peak height.
T_1	38	Spin-lattice relaxation time.
H_m	43	Amplitude of the local field modulation applied to the sample.
p	43	Frequency of the modulating field.
H	43	Instanteous value of the resultant magnetic field at the sample.
G_v	47	Incremental negative conductance appearing at the transitron terminals.
λ	59	*Linewidth of the N.M.R. absorption signal between the inflexion points of the line-shape function.
m_f	62	Index of modulation for a frequency modulated N.M.R. detector.

(*N.B. The 'linewidth' of the N.M.R. absorption signal may be defined in a number of ways of which two are given above. However the context in which each is used should dispel any confusion as to which term is implied.)

I - INTRODUCTION

I.1 Time Stability of the Field of an Electromagnet

The fluctuations of the field that may be expected to be encountered in a large electromagnet may, for convenience, be classified under three main categories namely:

(i) fluctuations at specific frequencies

(ii) slow drift

(iii) random fluctuations.

Field fluctuations at specific frequencies originate from the voltage output ripple of the power unit used to energise the magnet. The output ripple is characteristic of the type of power unit used, but the degree to which the ripple penetrates into the field is governed by the response characteristics of the magnet itself.

Electronic power supplies, which are used to energise high-voltage-low-current magnets, have an output ripple at a multiple of the A.C. mains frequency. At such high frequencies the effect of the ripple on the magnet field is negligible. When this is not the case it is usually possible, without appreciable loss of power, to employ appropriate filter circuits to eliminate the undesirable ripple.

The output voltage of a motor generator set has ripple components at the rotor frequency and at multiples of the rotor frequency. At these low frequencies the effect on the magnet field may be appreciable, and the use of

filter circuits may be rendered impracticable because of the large capacitors and high current-carrying inductors required.

Random fluctuations may occur due to changes in A.C. mains voltage or frequency, but may also originate from tube noise in high-gain D.C. amplifiers.

Slow changes in the static value of the magnet field may arise from corresponding changes in the A.C. mains supply, affecting the rotor speed.

The main source of slow drift is however, of thermal origin. Temperature changes can cause certain parameters in the whole stabilizing feed-back loop to vary e.g. output level of D.C. amplifiers.

In particular, variation of the ohmic load of the magnet itself produces a field drift of large magnitude.

A smaller, but not less important, field drift is that due to changes in magnet geometry and iron permeability produced by temperature changes.

I.2 Stabilisation Methods

Constant Current

There are many references in the literature to the stabilisation of the high-voltage-low-current type of electromagnet energised from a parallel bank of hard vacuum tubes.

Stabilisation is achieved by maintaining a constant current output and the methods employed have certain features in common with the wider problem of voltage stabilisation of electronic power supplies.

The method consists of comparing the voltage drop across a standard resistor, in series with the magnet against a reference voltage. The resultant voltage difference or error signal is then amplified and used to control the current output. The design problem centres on the method of achieving the very high D.C. gain required to produce the desired degree of stability.

High power electromagnets requiring an energising current of the order of 100 amperes have been operated from motor generator sets employing degenerative current feedback.

An error signal, obtained from the difference between a reference voltage and IR drop across a standard resistor, is amplified and used to control the field current of the generator.

However because of the large time constants involved, the feedback loop is unresponsive to the higher frequency fluctuations (e.g. ripple).

The magnitude of this ripple may be such as to block the high-gain D.C. amplifier and cause the whole feedback loop to become inoperative.

Methods of eliminating this undesirable ripple have been described by Sommers, Weiss and Halpem and by Wolff and Freedman.

I.3 Constant Field

The methods described above for stabilising a magnetic field rely on maintaining a constant current.

However, constant excitation alone will not ensure a constant magnetic field, for the field is also a function of the permeability of the iron and of the geometry of the magnet both of which are temperature dependent.

Therefore temperature changes will give rise to slow drifts of the magnetic field.

In order to stabilise a magnetic field directly, some means of detecting small changes in the value of the field is necessary.

One such method is to use a rotating coil placed in the magnetic field and to compare the induced e.m.f. against a reference voltage.

The disadvantages of this method is the difficulty of obtaining an alternating voltage sufficiently stable to act as reference.

Nuclear magnetic resonance affords a very sensitive means of detecting small changes in a magnetic field.

Packard has used the nuclear induction signal from protons in a water sample to produce a $\pm$ 75 volt change

for a ±0.3 gauss change of magnetic field. The additional information from this field discriminator was then used to augment the degenerative current feedback stabilisation of an existing electronic power unit.

Thomas has described an essentially similar NMR field discriminator which was used to control the field current of a generator and hence its output. The field of the associated electromagnet, it was claimed, was held constant to within 10% of the line width of the nuclear resonance absorption curve.

I.4 Analysis of a Feedback Control System

The block diagram of Fig. I.1 shows a basic feedback control system in which the controlled quantity C (modified by the feedback loop H) and the reference input R (which it is desired that C should emulate) are compared in some error detecting device. The resultant error signal E is amplified or otherwise manipulated by the forward loop G to produce the controlled output C.

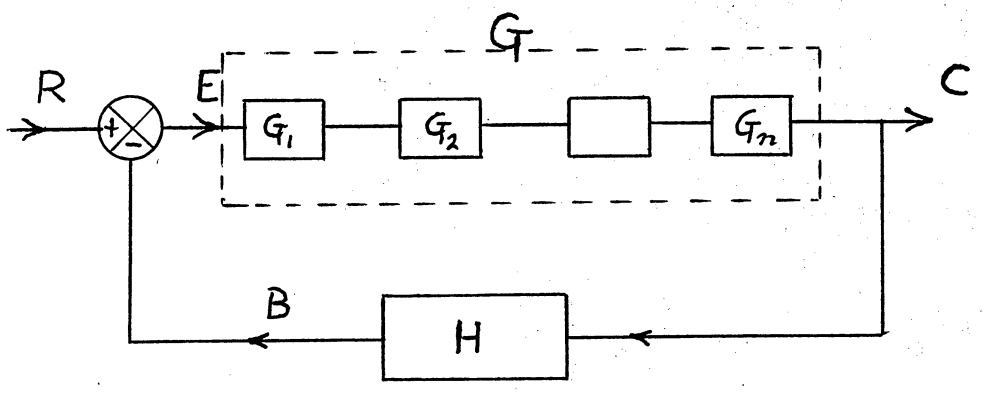

FIG I.1

It is assumed that each element of the forward loop may be described as a function of the frequency $\frac{\omega}{2\pi}$ by a transfer function (complex) of the type:-

$$Gr = K_r(j\omega)\frac{n(1 + j\omega\tau_{r1})(1 + j\omega\tau_{r2})\ldots}{(1 + j\omega\tau'_{r1})(1 + j\omega\tau'_{r2})\ldots}$$

where K_r is independent of frequency and $\tau_{r1}\ldots\tau_{rn}$ $\tau'_{r1}\ldots\tau'_{rn}$, are the time constants required to describe the given transfer function.

It is further assumed that each element in the loop is unilateral, so that the overall transfer function of the forward G loop is given by the product

$$G = G_1 \cdot G_2 \cdots\cdot G_n$$

Similar assumptions are made with regard to the transfer functions of the elements in the feedback loop H.

The equations of the system then become:-

$$\left.\begin{aligned} C &= GE \\ B &= HC \\ E &= R-B \end{aligned}\right\} \quad \ldots\ldots (I.1)$$

whence

$$\frac{C}{R} = \frac{G}{1 + GH} \quad \ldots\ldots (I.2)$$

I.5 Absolute Stability

A feedback control system containing linear elements is either stable of unstable. If the loop gain is sufficiently high there will exist some frequency for which the phase

shift is 180^{o} and the loop gain greater than unity, i.e. the feedback is positive. The system will then commence to oscillate with increasing amplitude which may either be self-destructive or which may reach a limiting value due to the introduction of non linear behaviour of certain elements in the loop causing the loop gain to become exactly unity.

From inspection of equation (I.2), it will be seen that instability will occur when the magnitude of $\frac{C}{R}$ tends to infinity. Hence the stability of a system may be investigated analytically by determining the roots of the equation $1 + GH = 0$. Graphical methods however are less tedious and physically more instructive.

A Nyquist diagram or polar plot in the complex plane of the open loop transfer function GH is shown in Fig. I.2 for a typical case.

The Nyquist criterion of stability for simple systems for which the function GH has no real, positive roots, may be related to the encirclement of the point $(-1, j0)$ by the locus of the vector GH over the frequency range $+\infty$ to $-\infty$.

If the nett encirclement is zero, the system is stable.

Alternatively the plot of GH in the form of log amplitude v. log frequency and phase angle v. log frequency graphs (Bode diagram: see Fig. I.3) may be used to predict the stability of a system. The simplified Nyquist stability criterion then requires the magnitude $|GH|$ should cross the

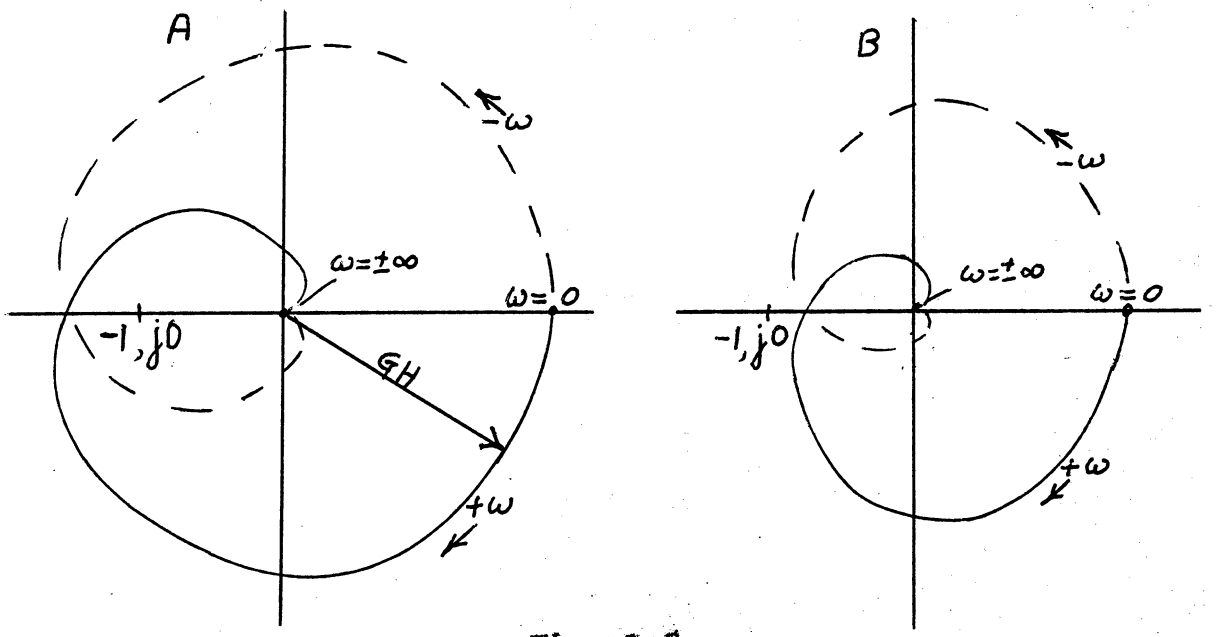

Fig. 1.2

A- Unstable System B- Stable System

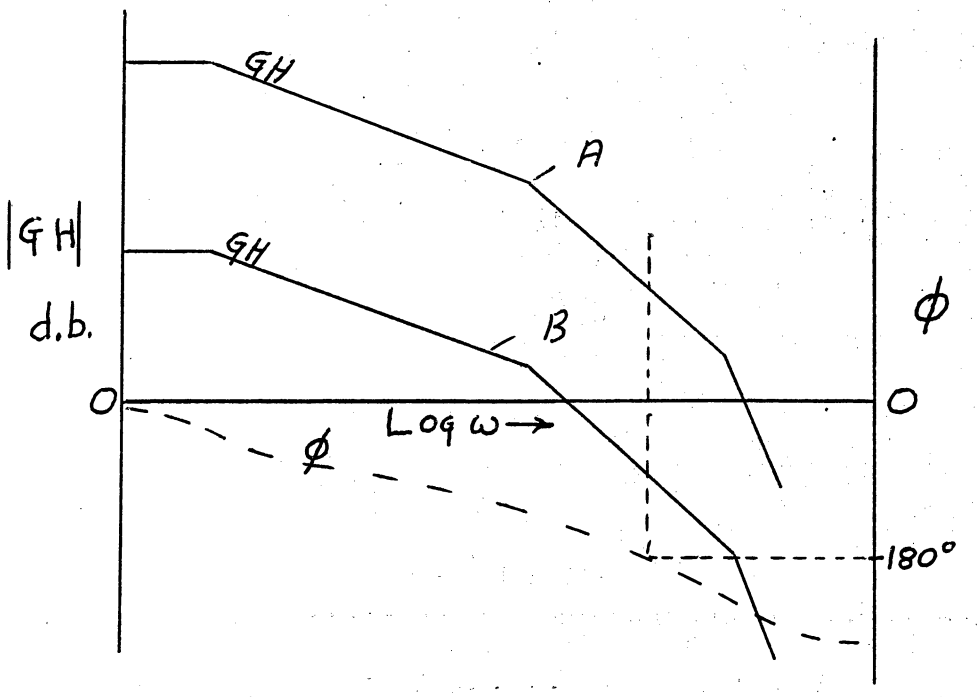

Fig. I.3

A- Unstable System B- Stable System

0 db axis at a frequency for which the phase angle is less than $\pm 180^{o}$.

In Fig. I.2 and Fig. I.3 are shown unstable systems which have been made stable by the simple expediency of reducing the loop gain. For most purposes this is of course most undesirable, and the stability of an otherwise unstable system is usually achieved by the reshaping of the locus of the transfer function in the neighbourhood of the point (-1, j0).

The shaping element is commonly inserted in the forward loop and is designed to modify the phase angle over the critical frequency range and to improve the frequency response at either low frequencies (phase lag circuits) or at high frequencies (phase advance circuits).

The relative stability of a system is described by the behaviour of controlled variable following a change of reference input or a system disturbance.

The controlled variable exhibits damped oscillation the maximum instantaneous error (R-C) or overshoot being a function of the rate of change of reference input. It may be shown that optimum performance is obtained when the transfer function GH suffers little attenuation at high frequency.

In a stabilization system which is subject to disturbances of large magnitude at low frequencies (e.g. slow drift) it is desirable, in order to keep the static error small, that GH should maintain a high value at a low or zero frequency.

These two requirements (good response at both high and

low frequencies) conflict both with each other and with the requirements for absolute stability, and the compromise between these requirements may form a major factor in the design of the complete feedback control system.

I.6 System Disturbances

The term disturbance here includes any change of parameter, noise or any undesired signal (e.g. ripple) injected into an element of the system.

The disturbance can be considered as an unwanted signal, U, injected into the system at a point immediately preceding the element in which the disturbance actually appears, as represented in the block diagram of Fig. I.4.

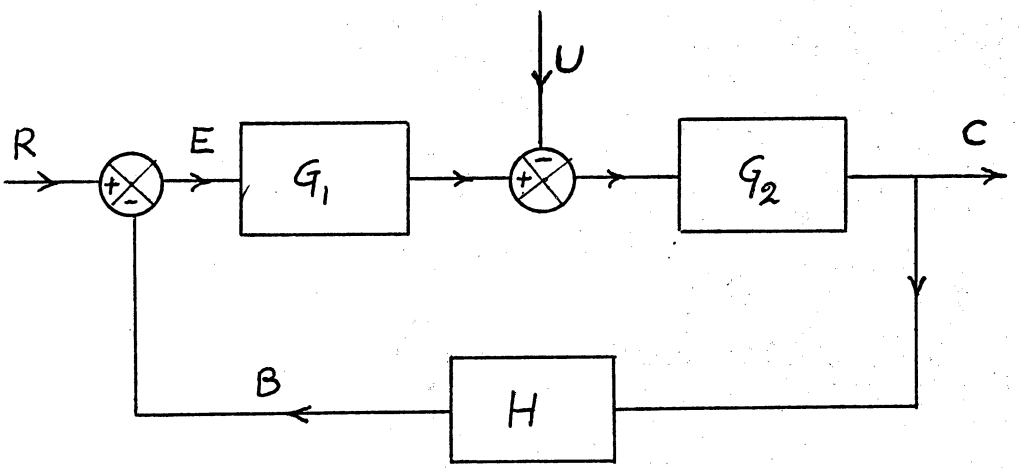

Fig. I·4

By applying the principle of superposition and regarding the reference input R as constant the equivalent circuit for variations in the controlled output Cu, due to the disturbance U, is shown in Fig. I.6.

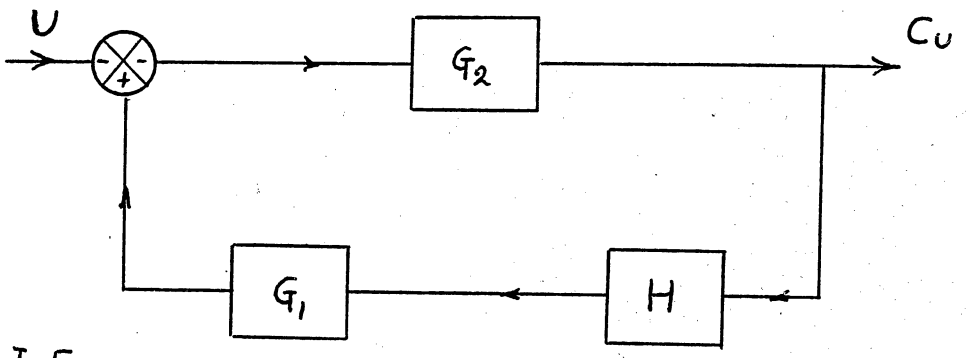

Fig I·5

Rewritting equation (I.2) in the notation appertaining to Fig.I.5 we have for the response of the controlled output Cu to a disturbance in the forward loop:-

$$\frac{Cu}{U} = \frac{G_2}{1 + G_1G_2H} \qquad \ldots\ldots (I.3)$$

while for the response of the controlled output C_R to the desired input, R (Fig. I.4 refers) we have:-

$$\frac{C_R}{R} = \frac{G_1G_2}{1 + G_1G_2H} \qquad \ldots\ldots (I.4)$$

Thus the ratio of desired to unwanted output is given by:-

$$\frac{C_R}{Cu} = \frac{R}{U} \cdot G_1 \qquad \ldots\ldots (I.5)$$

The above equations indicate that a high value of G_1 and a low value of G_2 at the frequency of the disturbance, are clearly desirable.

Thus, disturbances which originate near the output stage of the forward loop will be readily excluded, whilst the r everse is true for a disturbance originating near the input. A disturbance which actually appears at the input to the forward loop (i.e. $G_1 = 1$) will be indistinguishable from the reference input, i.e. such a disturbance will produce the same change in the controlled output as would an equal change of reference signal itself.

The effect of the frequency of the disturbance may also be obtained qualitatively from an inspection of equation (I.3). At low frequencies, such that the transfer functions suffer negligible attenuation or phase shift, and assuming $|G_1 G_2 H| > 1$ then

$$\frac{Cu}{U} \doteq \frac{1}{G_1 H} \quad .$$

Hence a large value of $G_1 H$ is desirable (consistant with the requirements of the absolute stability of the system) and the transfer function G_2, of that part of the forward loop succeeding the point of origin of the disturbance has negligible effect.

However at higher frequencies for which $|G_1 G_2 H| < 1$,

$$\frac{Cu}{U} \doteq G_2 \ ,$$

and the response of the controlled variable to the disturbance is the same as if the feedback loop were opened, i.e. the feedback loop is inoperative and ceases to produce degeneration of the disturbance at these frequencies.

As an example we may consider a ripple voltage injected into the system at some point. If the effect of the ripple on the controlled output is not negligible, it may be necessary to attenuate G_2 at ripple frequencies by the introduction of a filter element in the forward loop or by employing a subsidiary feedback loop on G_2 so as to produce the desired characteristics.

II - MAGNET AND GENERATOR CHARACTERISTICS

II.1 The Magnet

The design and performance of the University of New South Wales 18KW electromagnet have been discussed elsewhere, so that the following brief description will be a sufficient introduction.

The magnet, which is entirely iron-clad except for four access ports, is of cylindrical design with the yoke separable into two halves. Interchangeable pole-pieces of various shapes and diameters are provided and the air gap may be varied in increments of 1/8" from 1 3/4" to 4 3/4".

The main excitation coils total 1090 turns and are arranged in 10 pancakes which may be connected in series, parallel or any desired combination. Water-cooling labrinths between pancakes permit the dissipation of large powers without undue temperature rise.

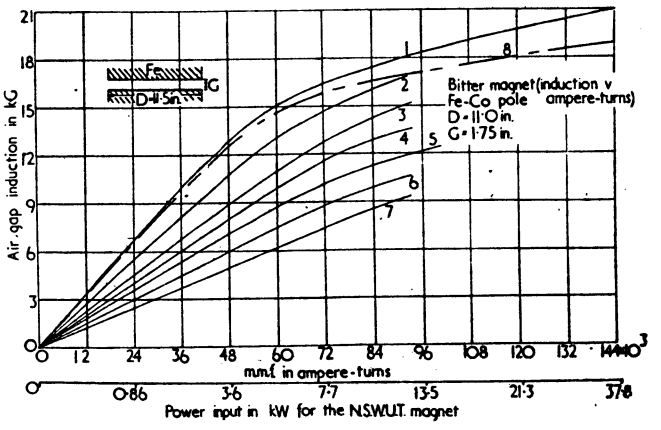

Fig. 14. Magnetization characteristics of N.S.W.U.T. magnet for 11·5 in. cylindrical poles

Curve 1, $G = 1{\cdot}75$ in.; curve 2, $G = 2{\cdot}25$ in.; curve 3, $G = 2{\cdot}75$ in.; curve 4, $G = 3{\cdot}25$ in.; curve 5, $G = 3{\cdot}75$ in.; curve 6, $G = 4{\cdot}75$ in.; curve 7, $G = 5{\cdot}4$ in.; curve 8, Bitter magnet (induction plotted against ampere-turns) Fe–Co pole $D = 11{\cdot}0$ in., $G = 1{\cdot}75$ in.

In addition, in each yoke half there is a pancake consisting of 2600 turns and having a resistance of 600 ohms. For convenience these are referred to as the "high impedance" coils.

In the subsequent experimental work (unless stated to the dontrary) it will be assumed that the magnet was operated under the following conditions:-

Pole-piece	-	11 1/2" diam. cylindrical
Air gap	-	2 1/2"
Main excitation Coils	-	all pancakes in series (resistance 2 ohms)

The D.C. excitation curves which are given in Fig. I.1 have been reproduced from the results of experiments of other workers.

II.2 The Generator : Characteristics

The magnet is energised from a motor generator set consisting of a 3-phase induction motor coupled to a 4-pole D.C. generator of conventional design.

The frequency response of the generator is primarily determined by the inductance and resistance of the generator field circuit, the inductance of the armature having negligible effect. In determining the frequency response it is essential therefore to employ the same circuits as would be used under normal operating conditions.

This circuit is shown in Fig. II.2 in which the generator field coils are fed from a bank of storage batteries (180V) in series with a power amplifier (parallel bank of vacuum tubes) which is shunted by a rheostat. (The circuit details of the power amplifier are given in Appendix B).

The rheostat enables the steady value of the field current to be set to any desired value in the range 0.5 - 5.0 amp., while the power amplifier provides for variations up to $\pm$0.5 amp.

The shunt resistor lowers the effective transconductance of the power amplifier but does not otherwise affect the operation of the forward loop.

Thus, the presence of a steady component of current in the generator field coils, due to the resistor and plate current of the power amplifier does not invalidate the feedback analysis of Section I for incremental operation if elements of the forward loop have linear characteristics over the operating range. After the desired steady value of current through the field coils has been obtained by adjustment of the rheostat and grid bias voltage of the power amplifier, any changes of current through the field coils, brought about by temperature changes etc, may be regarded as system disturbances originating at the input to the power amplifier.

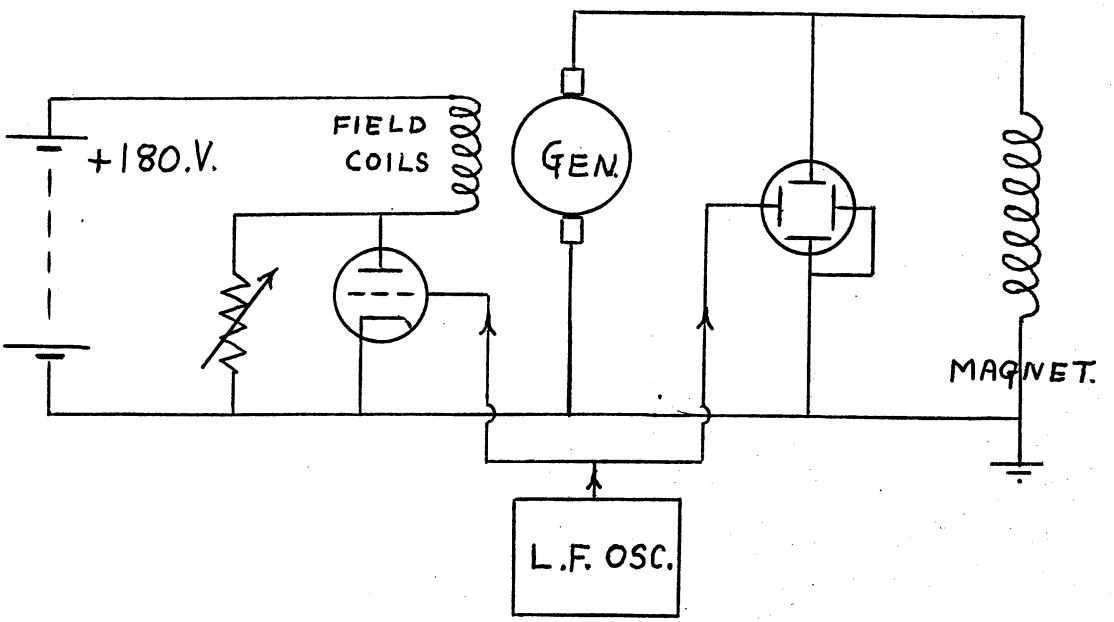

FIG II·2

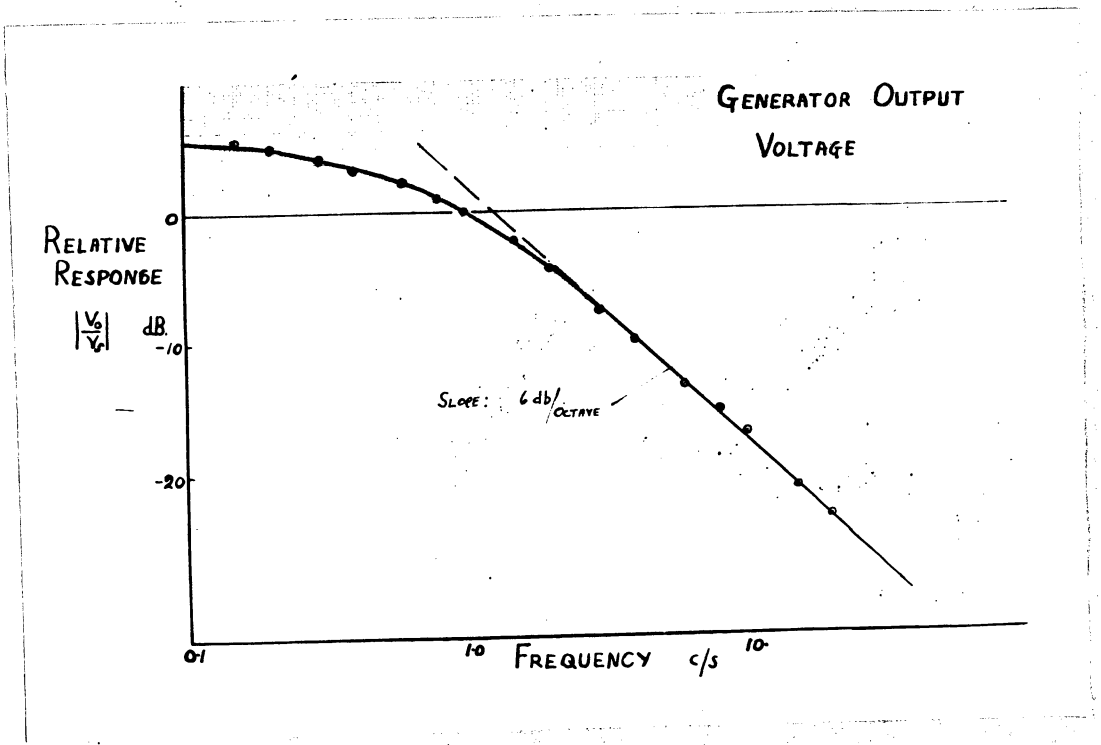

FIG II·3

The frequency response of generator under normal operating conditions was determined by applying a sinusoidal signal (v_i) from a low frequency oscillator to the grid of the power amplifier of the generator field circuit. The corresponding sinusoidal voltage (v_o) superimposed upon the direct voltage output was observed on a C.R.O. By applying a signal from the low frequency oscillator to the X-deflection plates of the C.R.O. an estimate of the phase shift as a function of frequency was obtained from the resultant Lissajous figures.

The results are shown in Fig. II.3 in which the relative response is shown plotted against log frequency with the relative response at 1 c/s arbitarilly taken as unity. The dotted curve represents the asymptotical plot of a transfer function G_g $(= \frac{v_o}{v_i})$:-

$$G_g = K_g \frac{1}{1 + w\tau_g}$$, which can be made to fit the experimental curve closely.

Thus the response of the generator may be represented by a transfer function of the type above having a single time constant $\tau_g = 0.26$ sec and amplification constant $k_g = 1.4$ (this is the incremental value over the operating range as determined from D.C. characteristics).

The frequency response of the output voltage of the generator is, of course, slightly dependent upon the nature of the load by virtue of the effects of armature reaction.

This however will be of no concern since the generator will always be presented with the same load, namely, the magnet.

II.3 Frequency Response of Magnet : Main Excitation Coils

The frequency response of the magnet was investigated in two steps namely

(i) the behaviour of the magnet current

(ii) the behaviour of the magnet field, to a sinusoidal voltage superimposed upon the direct voltage appearing at the magnet terminals.

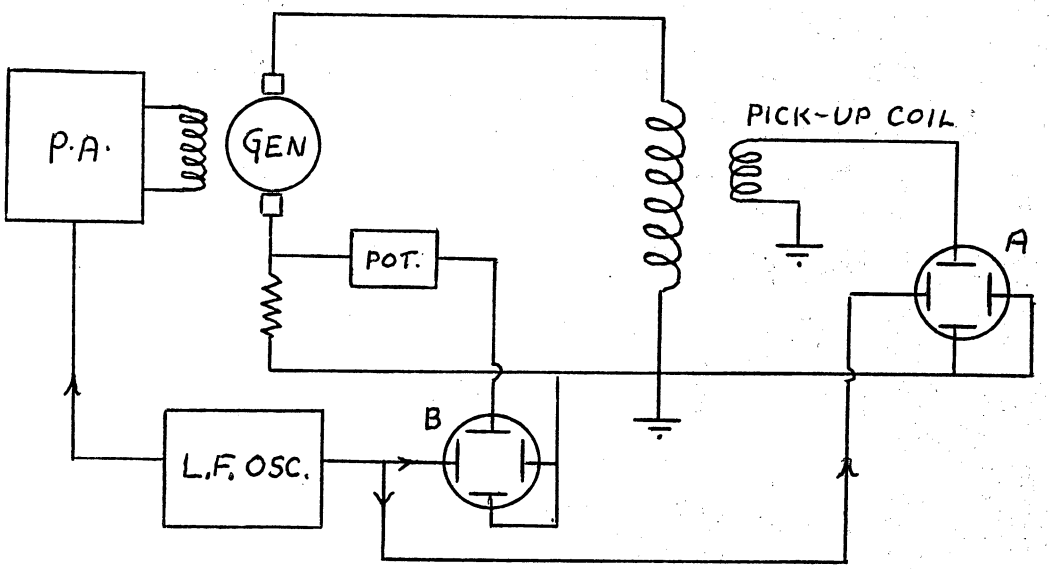

Fig. II.4

N.B. **The amplifier of C.R.O. "A" has a lower frequency limit of 0.15 c/s. C.R.O. "B" has a d.c. amplifier- hence the need for the "backing off" potentiometer.**

The behaviour of the magnet current was obtained from the IR drop across a small resistance inserted in series with the magnet. The D.C. component was backed off by means of a potentiometer, and the variations observed on a C.R.O. in the normal manner (Fig. II.4). The variations of magnetic field were obtained by means of a pick-up coil placed in the magnet air-gap.

The results of these two tests are plotted in Fig. II.5 and Fig. II.6 and show that a frequency of 1 c/s and above the response of the magnet current becomes constant i.e. the magnet behaves as a resistive load to sinusoidal variations of applied voltage. On the other hand the response of the magnet field continues to fall at a rate of 6 db. per octave.

The frequency range of these tests are unfortunately limited, at the one end by the lowest frequency of the low frequency generator (0.1 c/s) and at the other end by the attenuation at high frequencies which causes the variations of current and field to be obscured by effects of the ripple in the generator output.

However, the results in general agree quite well with the behaviour which may be deduced from a very simple model of the effects of eddy currents in the magnet (Appendix A).

This treatment gives the following expressions for the transfer functions:-

$$G_i = \frac{i}{V} = \frac{1 + j\omega\tau_e}{R_m(1 + j\omega(\tau_c + \tau_e))}$$

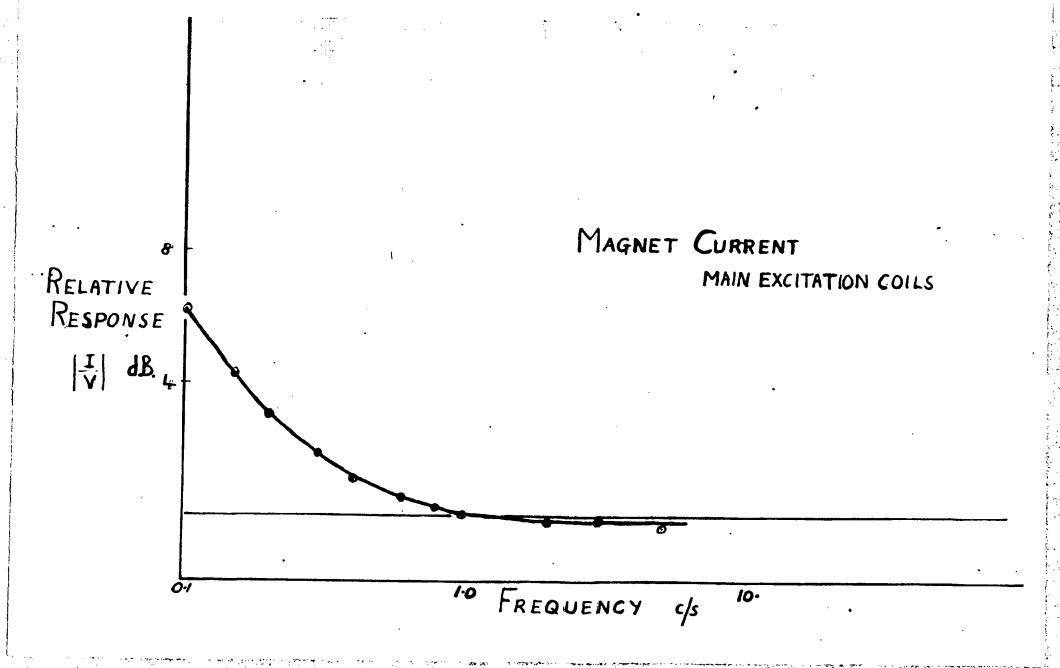

FIG II·5

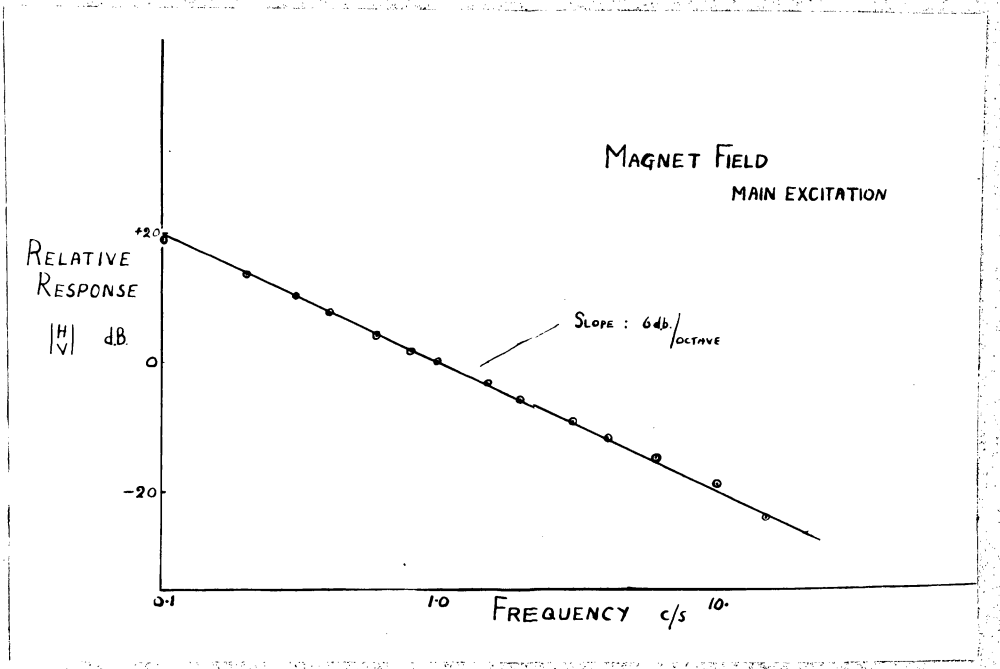

FIG II·6

$$G_m = \frac{H}{v} = K_m \cdot \frac{1}{1 + j\omega(\tau_c + \tau_e)}$$

where: v,i and H are the sinoidal variations of applied voltage, magnet current and field respectively;

τ_c and τ_e are the time constants associated with the magnet coils and circulating eddy currents;

R_m is the ohmic resistance of the magnet;

$K_m = \frac{C}{R_m}$, C being the D.C. excitation constant of the magnet ($\sim$290 gauss.amp.$^{-1}$)

By fitting the experimental results to the theoretical expressions, we obtain the following values:-

$$\tau_c = 1.7 \text{ sec.} \qquad \tau_e = 0.8 \text{ sec.}$$

We note that the impedance looking into the magnet terminals $Z_m = \frac{v}{i} = \frac{1}{G_i}$. Thus for frequencies for which $\omega\tau_e > 1$, we obtain :-

$$Z_m = R_m \cdot \frac{(\tau_c + \tau_e)}{e}$$

Using the above values for τ_c and τ_e gives

$$Z_m = 3.1\ R_m$$

which agrees with direct experimental observations for frequencies above 1 c/s.

We may summarise by stating that, to a good approximation, the response of the magnet field to a voltage applied to the magnet terminals may be represented by the transfer function :-

$$G_m = K_m \cdot \frac{1}{1 + j\omega\tau_m}$$

where τ_m = 2.5 sec. $\qquad K_m$ = 145 gauss.~~amp.~~ volt^{-1}

II. 4 High Impedance Coils

The frequency response of the high impedance coils has been investigated in a circuit which simulates normal working conditions (Fig. II.7). A sinusoidal signal from a low frequency generator (v_s) is applied to the grid of a power amplifier which contains a high impedance coil as plate load. The resultant variation in magnetic field is obtained by means of a pick-up coil placed in the air-gap.

The relative response, which is plotted in Fig. II.8, shows a somewhat complicated behaviour consisting of three (or more) time constant terms.

It will be observed that at low frequencies the attenuation rate is 6db/octave while for higher frequencies attenuation is at the rate of 12 db/octave.

Although no theoretical analysis has been undertaken, the 6db/octave attenuation at frequencies below 1 c/s is indicative of close coupling between the high impedance coils on the one hand and the induced eddy currents and main excitation coils on the other. At low frequencies therefore, the response of the high impedance coils is essentially that of the magnet itself.

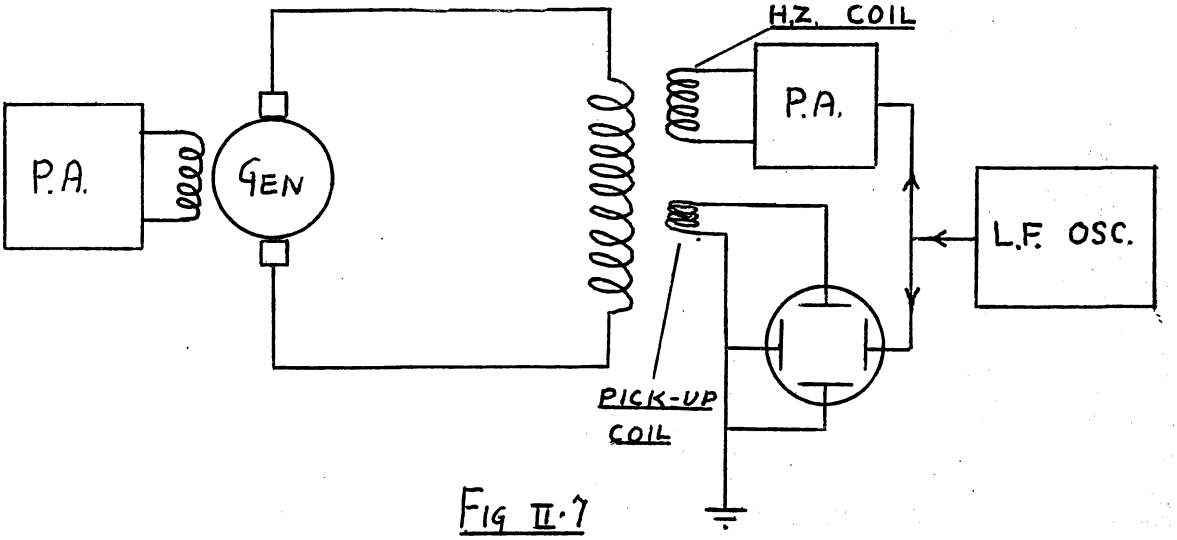

FIG II·7

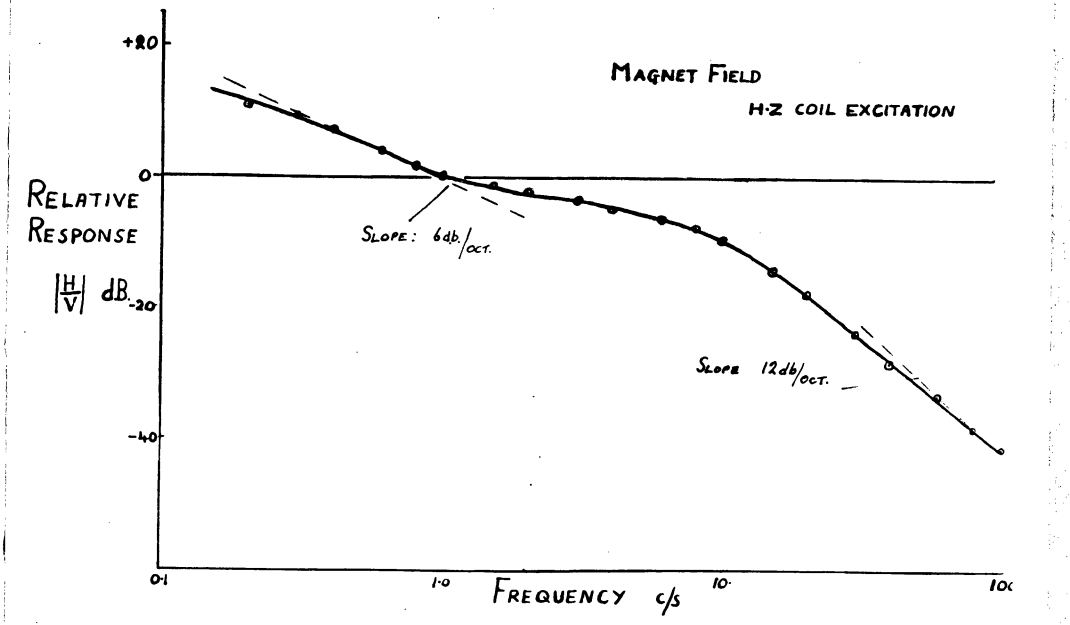

FIG II·8

II.5 Magnet Field Fluctuations

With the magnet supplied directly from the motor generator, the magnet field is subject to fluctuations as described below. The magnitude of these fluctuations was estimated from the behaviour of the absorption signal of a nuclear magnetic resonance detector (Section IV).

The voltage output of the generator contains ripple components at the rotor frequency (12.5 c/s approximately) and at the fourth harmonic (~50 c/s).

The magnitude of the ripple at these frequencies is such that in spite of the large time constant of the magnet, their effect on the field is significant

Generator $^{o}/_{p}$: 40 volts Magnetic Field 6000 gauss

Ripple Frequency	Ripple Voltage	Ripple Field
12.5 c/s	250 mV. RMS	0.5 gauss p-p
50 c/s	100 mV. RMS	$<$ 0.1 gauss p-p

Other ripple components (e.g. commutator) produce no observable effect on the magnet field because of their high frequency and/or small magnitude.

After the initial "warming-up" period (during which the drift of magnetic field may be quite large) it is possible to distinguish two further types of field fluctuation.

The slow drift, of thermal origin, has a typical value of a few gauss per minute. Superimposed upon this, there exists a random fluctuation which exhibits some degree of

hidden periodicity: such fluctuations may have an extreme value up to one gauss per second. While an exact analysis of this type of fluctuation has not been undertaken, there appears to be some correlation between it and an observed small axial motion of the generator armature. The effects of the field fluctuations described above may be observed in the oscillograms of Figs. IV.12 and 13.

II.6 Possible Stabilising System

Since it is desired to maintain a constant magnetic field rather than a constant excitation current, it was decided to stabilise the magnetic field by a nuclear magnetic resonance discriminator which would provide a correction signal that could be applied to the power amplifier of the generator field circuit in such a manner as to maintain a constant field.

Such an arrangement, as it stands, would not however prove workable.

In the first instance, because of the large time constants involved (generator and magnet) the feedback loop would cease to correct for fluctations above a certain frequency e.g. for the 12.5 c/s ripple, due to generator and magnet alone the response is down by approximately 70db.

Increasing the loop gain in an attempt to provide some correction at these frequenices will cause the feedback loop as a whole to become unstable.

Furthermore, as will be discussed in Section V, if the

residual fluctuations are greater than the line width of the nuclear magnetic resonance absorption signal, (which is of the order of 0.3 gauss) the discriminator will cease to function altogether.

It is therefore obvious that some additional means of smoothing the magnetic field must be provided. If this can be accomplished so that the more rapid fluctuations are reduced to a value less than the line width of the nuclear magnetic absorption signal, then the feedback loop will be able, with carefull design, to correct for slow drifts, which would otherwise produce changes of up to 10% of magnet field.

III SMOOTHING THE MAGNET FIELD

III.1 Ripple

The first attempts to eliminate the output voltage ripple of the generator employed degenerative feedback through the generator field coils.

The ripple in the generator output was fed through a blocking condenser to an amplifier and thence to the input of the power amplifier in the generator field circuit. Using wide-band amplification, the loop was unstable and oscillation occurred unless the amplifier gain was reduced to a very low value.

A selective filter tuned to the frequency of the predominant ripple 12.5 c/s was therefore inserted in the loop together with a phase shifting network. (Block diagram Fig. III.1). By adjustment of gain and phase shift the

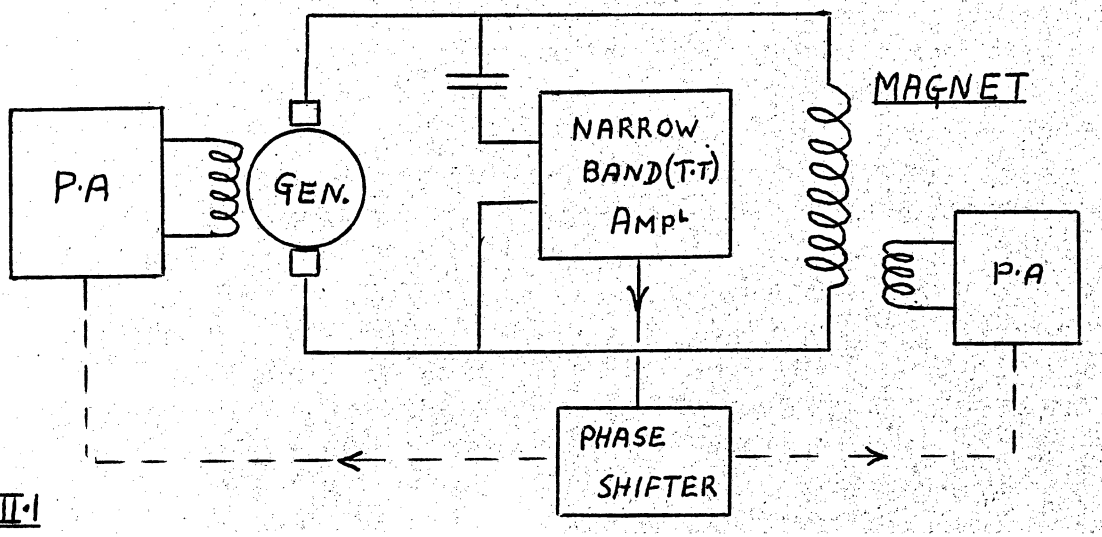

Fig III.1

optimum results obtainable were thereduction of the 12.5 c/s ripple by a factor of 2 approximately with the introduction of some additional ripple at the second harmonic frequency.

The second method attempted to counter-act the ripple in the magnet itself by producing field by means of a subsidiary high impedance coil, a field variation in anti phase to that produced by the ripple current flowing in the main excitation coils.

This was accomplished by feeding the ripple voltage from the generator output, after selective amplification and phase-shift, to the grid of a power amplifier which contained the high impedance coil as plate load.

With the amplifier gain and phase shift adjusted to give optimum correction, the 12.5 c/s component of the ripple was reduced from 2/3rd to approximately 1/10th of the line width of the nuclear magnetic resonance absorption signal, i.e. to .03 gauss peak to peak.

Although a complete stabilisation system has been operated incorporating this method of reduction of ripple, the performance was not considered entirely satisfactory. There still existed some residual fluctuation due to ripple components which were not corrected for by this circuit which was selective to 12.5 c/s only.

The third method adopted employs what is essentially a filter consisting of a choke of large current carrying capacity in the form of the primary windings of a 35 KVA 3-phase transformer which is inserted in series with the magnet, and a bank of four 6AS7 tubes which are connected across the

magnet terminals. The direct voltage across the magnet terminals ($\sim$ 50V) acts as the plate supply for these tubes which operate satisfactorily at this voltage.

The ripple voltage existing at the magnet terminals is fed through a blocking condenser and two stage amplifier to the grids of the power tubes. Fig. III.2 gives a block diagram while circuit details are given in the appendix

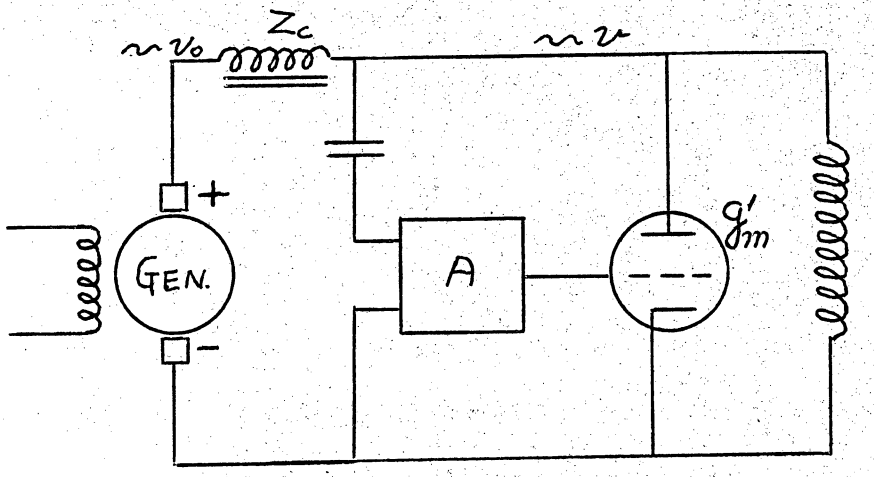

FIG III·2

A simple analysis shows that the bank of power tubes with preamplifier acts as an impedance $\frac{1}{Ag_m'}$ which may be made small compared with the impedance of the magnet, so that if v_o is the ripple voltage at the generator output, the ripple voltage v occurring across the magnet terminals is given by

$$\frac{v}{v_o} = \frac{1}{1 + Zcg_m'A}$$

where Zc = impedance of choke at the ripple frequency

g_m' = effect transconductance of the bank of power tubes

A = amplification of pre-amplifier.

The attentuation thus effected is a function of the frequency of the ripple component and is limited by the inductance of the choke which in turn restricts the maximum current that may be used before the onset of saturation effects in the core of the choke.

By this method the ripple voltage at 12.5 c/s measured across the magnet terminals was reduced by a factor of 20, with a proportionate increase in attentuation at higher frequencies.

The effect of any residual ripple voltage on the magnet field was thus rendered negligible compared with the line width of the nuclear magnetic resonance absorption signal.

III.2 Random Fluctuations

The use of an end-stop bearing on the rotor shaft had some effect in reducing the magnitude of the random fluctuations, thus confirming that some correlation existed between this fluctuation and the axial motion of the rotor described in Section II

The end-stop bearing took the simple form of a 3/4" diam. ball bearing engaging in a conical hole at one end of the rotor shaft, and held firmly against the rotor shaft by means of an adjustable vertical steel plate.

The remaining random fluctuations were reduced to proportions which could be accommadated by the main nuclear magnetic resonance feed-back loop, by a rate-of-change subsidiary feedback loop as shown in Fig.III.3.

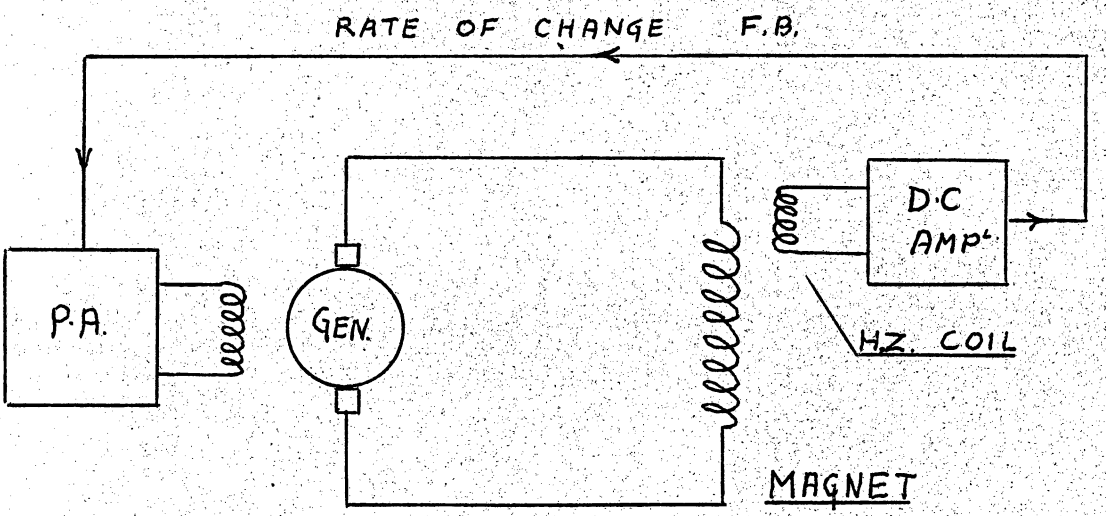

FIG III.3

The second high impedance coil is used as a pick-up coil and generates a voltage which is proportional to the rate-of-change of magnetic field. This voltage after D.C. amplification is applied in phase opposition to the input of the power amplifier of the generator field circuit.

The actual circuit of Fig.III.3 is represented in block diagram form in Fig. III4 which in turn may be simplified to that given in Fig.III.5 by an elementary theorem of servo-mechanism theory which states that an element G having a subsidiary feed-back loop H is equivalent to a single element having a transfer function G' given by

$$G' = \frac{G}{1 + GH} \qquad \ldots\ldots (III.1)$$

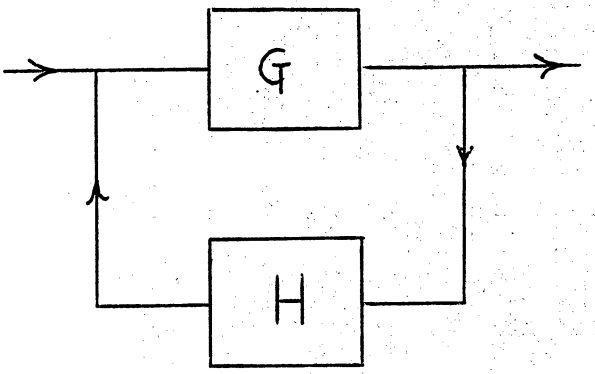

Fig III.4

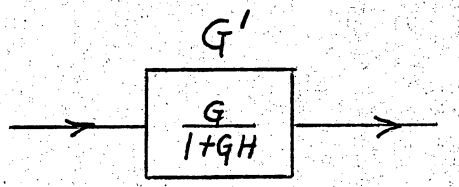

Fig III.5

In our case G is the product of the transfer functions of generator and magnet:-

$$G = G_g \cdot G_m = \frac{K_g}{1 + j\omega\tau_g} \cdot \frac{K_m}{1 + j\omega\tau_m}$$

and H being proportional to the rate-of-change is represented by a transfer function of the type:-

$$H = jK_r\omega$$

where K_r is a constant depending on the area turns of the pick-up coil and the amplification obtained in the D.C. amplifier.

Thus

$$G' = \frac{\dfrac{K_g \cdot K_m}{(1 + j\omega\tau_g)(1 + j\omega\tau_m)}}{1 + \dfrac{jK_r\omega \cdot K_g K_m}{(1 + j\omega\tau_g)(1 + j\omega\tau_m)}} \quad \ldots (III.2)$$

Although an exact analysis of equation (III.2) is both long and tedious, a qualitative explanation of the behaviour of the

rate-of-change feed-back loop may be obtained from a consideration of equation (III.1).

At very low frequencies, $H \rightarrow 0$, and again at very high frequencies $G \rightarrow 0$. In both cases $|GH| \ll 1$ and $G' \rightarrow G$.

Hence at very low and very high frequencies the rate-of-change feed-back loop has negligible effect.

Over an intermediate frequency range for which $|GH| \not< 1$, $|G'| < |G|$, i.e. the rate-of-change feed-back loop produces greater attenuation. Hence to a first approximation, its effect may be described as that of increasing the time constant of the system.

This has been checked experimentally by applying a small step-function of voltage to the grid of the power amplifier of the generator field circuit and observing the rate-of-change of magnetic field by timing the motion of a nuclear magnetic resonance signal displayed on a C.R.O. The effect of the rate-of-change feed-back loop, thus observed, was to increase, by a factor of 12, the time taken for the magnetic field to change by 2/3rd of the total change produced by the application of the step voltage input.

With the ripple filter and the rate-of-change feed-back loop in operation, residual fluctuations are either negligibly small or occur at such a slow rate that they should be capable of being corrected for by a "slow drift" feed-back loop employing a nuclear magnetic resonance field discriminator.

IV - DETECTION OF THE N.M.R. ABSORPTION SIGNAL

I. Introduction

The basic principles of N.M.R. (nuclear magnetic resonance) have veen described elsewhere (Block; Purcell) and it will be sufficient, for the purpose of describing the operation of the N.M.R. detectors below, to recall that when a sample of nuclear spins is placed in a magnetic field H_o, and a small r.f. field $2H_1 \cos\omega_o t$ is applied at right angles to H_o, nuclear magnetic resonance occurs when H_o has the value H^* given by

$$H^* = \frac{\omega_o}{\gamma} \qquad \ldots\ldots (IV.1)$$

where $\frac{\omega_o}{2\pi}$ is the frequency of the applied r.f. field, and γ is the gyro-magnetic ratio for the sample nuclei (for the porton $\gamma = 2.672 \pm .006 \times 10^4$ rad.sec^{-1}gauss^{-1}).

If the sample is enclosed in a coil supplied from an r,f, source, the effect of the nuclear magnetic resonance may be described as producing a change in the flux (due to the precessing nuclei) which is linked with the coil. This change in flux through the coil at resonance is equivalent to a change in the inductance of the coil. It may be shown that at resonance the inductance of the coil may be represented by

$$\mathcal{L} = L_o(1 + 4\pi\zeta\chi) \qquad \ldots\ldots (IV.2)$$

where $\chi = \chi' - j\chi''$ is the nuclear susceptibility of Block's semi-macroscopic theory ζ is the filling factor of the sample within the coil. L_o is the inductance of the coil in the absence of nuclear magnetic resonance.

Now the impedance of the coil is given by

$$\mathcal{Z} = r + j\omega\mathcal{L} = r + j\omega L_o(1 + 4\pi\zeta\chi)$$

$$= r + j\omega L_o(1 + 4\pi\zeta(\chi' - j\chi''))$$

$$= r + 4\pi\zeta\omega L_o\chi'' + j\omega L_o(1 + 4\pi\zeta\chi') \quad \ldots (IV.3)$$

Hence there is an effective increase in resistance, δr, of the coil (representing the absorption of r.f. energy at resonance) which is given by

$$\frac{\delta r}{r} = \frac{4\pi\zeta\omega L_o\chi''}{r} = 4\pi\zeta\chi''Q \quad \ldots\ldots (IV.4)$$

This is accompanied by a change in inductance δL_o given by

$$\frac{\delta L_o}{L_o} = 4\pi\zeta\chi' \quad \ldots\ldots (IV.5)$$

If the coil forms part of a tuned circuit, the resonant impedance, which is purely resistive, is

$$Z = Q\omega L_o = \frac{\omega^2 L_o^2}{r}$$

and for small changes we have:-

$$\frac{\delta Z}{Z} = -\frac{\delta r}{r} + 2\frac{\delta L_o}{L_o}$$

$$= -4\pi\zeta\chi''Q + 2(4\pi\zeta\chi')$$

Since, $Q \gg 1$ (in general practice $Q \sim 100$) we have

$$\frac{\delta Z}{Z} = -4\pi\zeta\chi''Q \quad \ldots\ldots (IV.6)$$

When the coil is supplied with its r.f. energy from a constant current source, the change in r.f. voltage, v, across the coil that occurs at resonance is given by

$$\frac{\delta v}{v} = \frac{\delta Z}{Z} = -4\pi\zeta\,\chi''\,Q \qquad \ldots\ldots\ldots (IV.7)$$

In a similar manner it may be shown that the phase of r.f. voltage changes by an amount $-4\pi\zeta\,\chi' Q$.

Thus a phase sensitive device will detect the dispersion component of the nuclear induction signal, where as, in order to observe the absorption signal, an amplitude-sensitive device is required.

It is the latter case that we shall be concerned with and the theory shows that in the absence of saturation, the maximum value of χ'' is $\frac{1}{2}\chi_o\omega_o T_2$ and the maximum change in amplitude of the r.f. voltage across the coil is therefore

$$(\delta v)_{max} = 2\pi\,\chi_o\omega_o T_2\zeta Q.v \qquad \ldots\ldots (IV.8)$$

where χ_o is the static susceptibility of the sample and T_2 is the spin-spin or transverse relaxation time and is related to the spread of field ~~expressed~~ experienced by the ensemble of nuclei in the sample.

From the precise definition of T_2, it may be shown that

$$T_2 = \frac{2}{\gamma.\,\Delta H}$$

where ΔH is the line width of the absorption curve at half peak height. Thus since the curve is normalised, it follows that the peak height is inversely proportional to the line-width, and that a magnetic field of good homogeneity is required in order to obtain a recognisable signal.

From equation (IV.8) we note that besides the radio frequency ω_o and the Q of the coil the signal strength is

proportional to the r.f. voltage v across the coil. However v may not be made too great because of a saturation effect which occurs when the r.f. field H_1 becomes too large. The saturation effect may be described by a saturation factor $1 + \gamma^2 H_1^2 T_1 T_2$ where T_1 is the spin-lattice relation time and we require that $\gamma^2 H_1^2 T_1 T_2 \ll 1$.

If T_1 is large, it may be artificially reduced, in the case of liquids, by using a paramagnetic salt as a solute; this allows the amplitude of the r.f. field H_1 to be increased without saturation and thus improves the signal to noise ratios for otherwise weak signals. Thus for the proton N.M.R. detectors described in this section, the sample takes the form of an aqueous 0.1 molar solution of ferric nitrate.

IV.2 The Amplitude Bridge

The early methods of Block and of Purcell for the detection of N.M.R. do not lend themselves to either field measurement or field control, inspite of their good noise figures, because of their complexity, microphony and the critical adjustment or tuning required. A number of methods employing bridge circuits or oscillators have since been devised and two such methods have been employed in conjunction with the field measurement and stabilisation of the University of New South Wales magnet.

The circuit of the amplitude bridge, which is given in Fig. IV.1, was first described by Thomas and Huntoon.

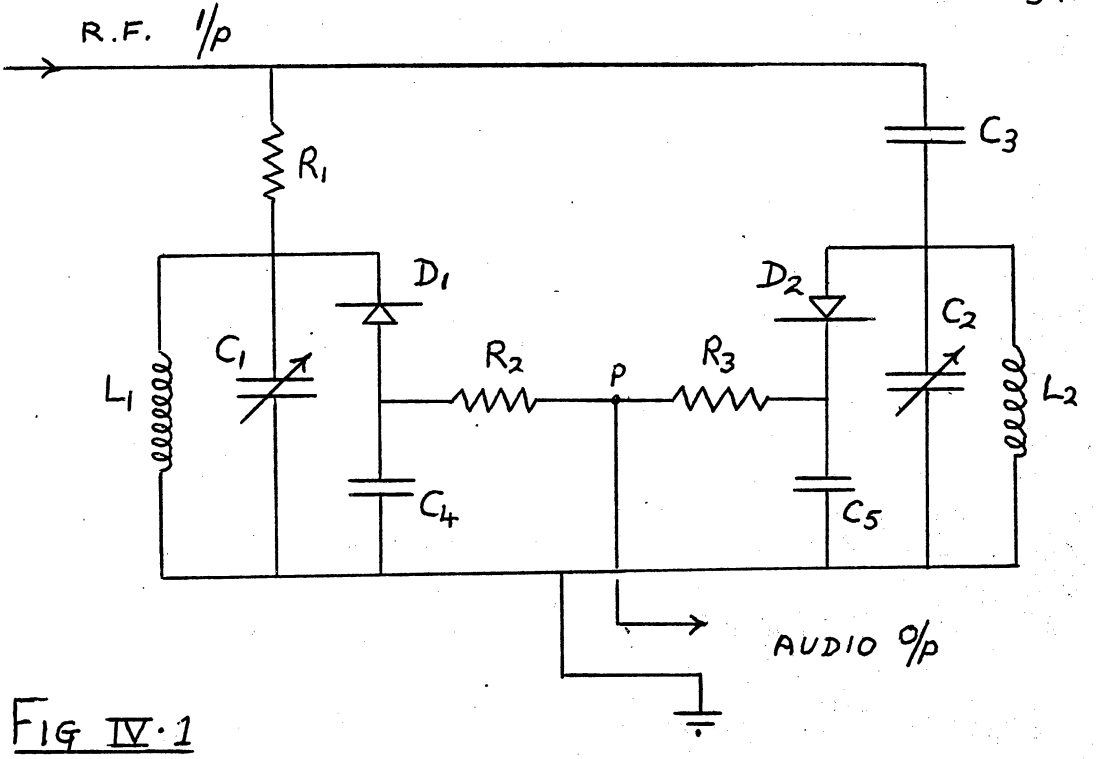

FIG IV·1

The coil L_1, containing the sample, forms a tuned circuit with the variable condenser C_1 and is energised from a signal generator through a resistance R_1 which is large compared with the resonant impedance of the tank circuit, in order to simulate a constant current source for the tank circuit.

The condensers C_2 and C_3 form a potential divider with the r.f. choke L_2 acting as a D.C. path for the diode D_2. The r.f. voltages across the tank circuit and condenser C_2 are rectified by the diodes D_1 and D_2 respectively and the difference signal occurring between the point P and earth is subsequently amplified and displayed on a C.R.O.

The bridge is balanced by employing 400 c/s amplitude modulation of the r.f. input from the signal generator and adjusting C_2 so that the magnitude of the detected 400 c/s

appearing in the output is a minimum.

In normal operation (no 400 c/s modulation of the r.f.) with the bridge balanced, noise and hum modulation of the r.f. appearing in the output of the signal generator will be balanced out by the bridge and will not appear in the detected output. The changes in amplitude of the r.f. voltage across the tuned circuit that occur under magnetic resonance conditions will however be rectified by the diode D_1 and will appear in audio output.

IV. 3 Design Modifications

The circuit of Fig. III.1 did not however prove satisfactory in practice and many unsuccessful attempts were made to obtain a N.M.R. signal. The following modifications were found necessary.

(i) It was estimated that, for an optimum N.M.R. signal with the sample remaining unsaturated, a maximum r.f. voltage across the sample coil of approximately 2V. r.m.s. was required. This necessitated an r.f. input of at least 10V. r.m.s. which was not procurable from the signal generator employed.

A single stage tuned-anode r.f. pre-amplifier was therefore designed and constructed to provide the necessary voltage input to the bridge.

(ii) The noise level in the output was found to be above the expected level of the N.M.R. signal. Other sources

of noise (e.g. dry joints, etc.) having been searched for and eliminated, it was discovered that the crystal diodes used (1N38) were excessively noisy.

An immediate improvement in the noise level was obtained when the crystal diodes were replaced by hard vacuum tubes (1S5). However, before a satisfactory balance could be obtained, it was found necessary to reduce the capacitance to earth of the diode tube D_2 by careful mounting and to shield the 1.5V dry cells (used for the filament supplies of the diode tubes) from each other and from the remainder of the circuit, in order to eliminate undesirable mutual coupling between the two halves of the bridge.

(iii) Care had to be taken in choosing the valves of C_2 and L_2 to ensure that over the frequency range used, L_2 and C_2 did not approach the formation of a resonant circuit.

At one stage the capacitors C_3 and C_2 were replaced by two fixed resistors. This arrangement proved inflexible in tuning the bridge for balance and the original capacitor form of potential divider was reverted to. However, in order to provide for fine adjustment in balancing the bridge an additional variable resistor R_4 was inserted between R_2 and R_3.

The constructional details of the modified version of the amplitude may be seen in Fig. IV.2.

The preliminary experiments to obtain a N.M.R.

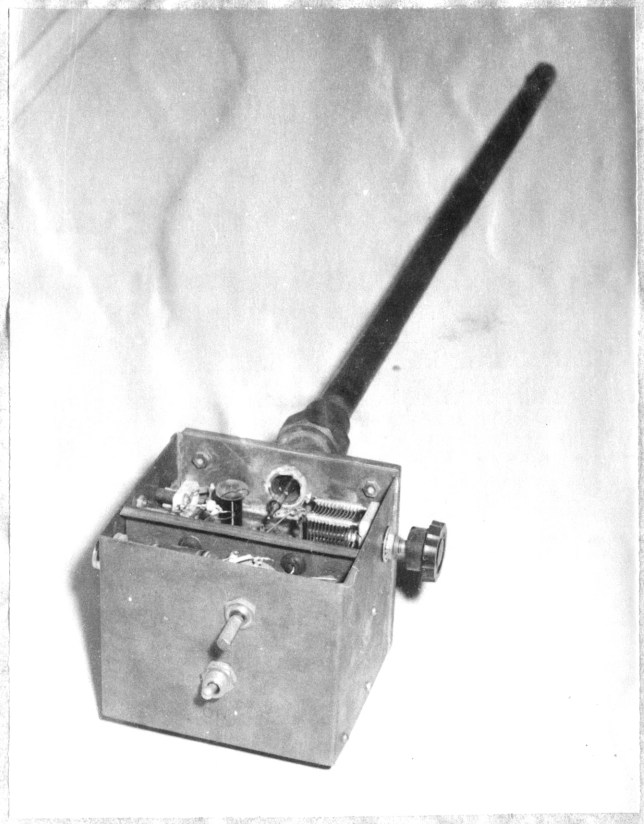

Fig. 1V.2(A) (left)

Fig. 1V.2(B) (below)

Constructional details of the Amplitude Bridge.

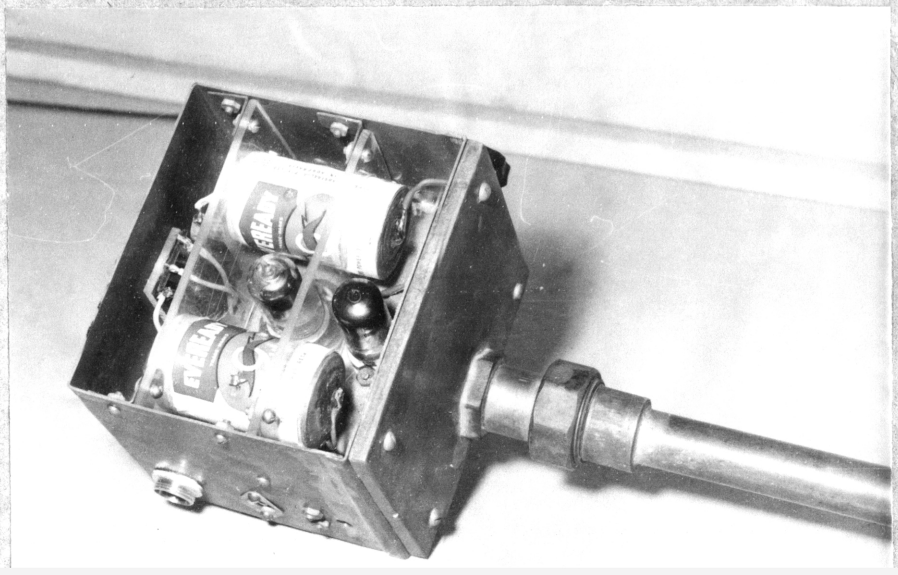

absorption signal with the amplitude bridge using a small laboratory electromagnet proved at first unsuccessful. This was ultimately found to be due to the poor homogeneity of the field of the electromagnet. In order to obtain a sufficiently high field (4,000 gauss), the original air-gap of the magnet had been reduced from 1 3/4" to 7/8" by the insertion of a cylindrical piece of mild steel. By turning down the central portion of one face of the cylinder leaving a circumferential lip approximately 0.02" thick and 0.2" wide, the homogeneity at the centre of the air-gap was sufficiently improved so that a N.M.R. signal was immediately obtained.

IV.4 Practical Performance of Amplitude Bridge

The bridge has been used for initial measurements of field pattern and homogeneity of the 18 K.W. University of New South Wales magnet, a block diagram of the apparatus employed being shown in Fig. IV.3.

The Helmholtz coils provide a local modulation of the D.C. magnetic field H_o, such that the instantaneous value of the field at the sample is

$$H = H_o + H_m \sin pt$$

where H_m and $\frac{p}{2\pi}$ are the amplitude and frequency of the modulating field.

If $|H^* - H_o| < H_m$, the sample will pass through the resonant field H^* twice during one modulation cycle (Fig. IV.4). When a voltage in phase with the modulation

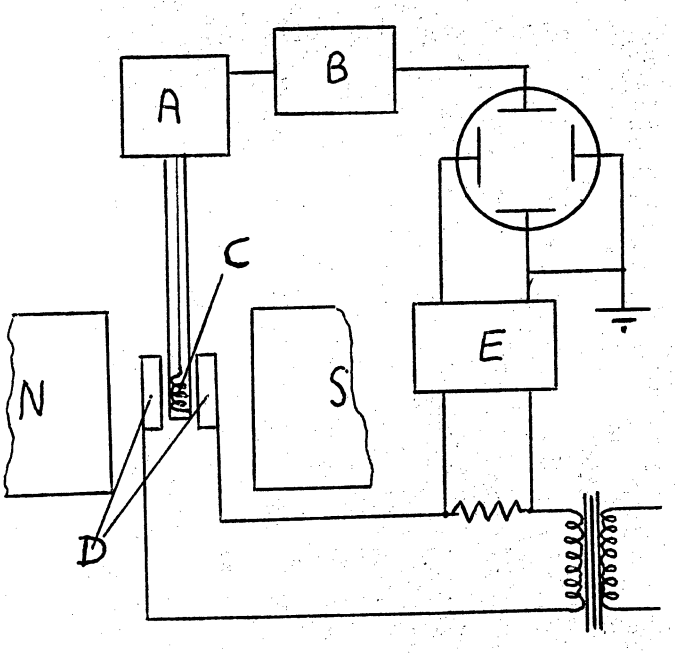

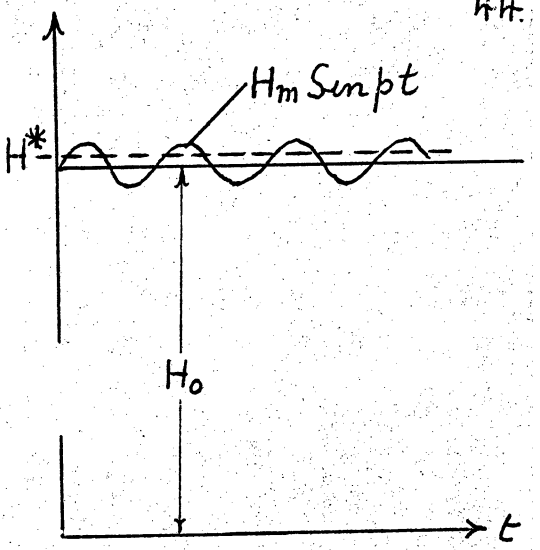

Fig. 1V.4

A- Amplitude Bridge
B- Amplifier
C- Sample coil
D- Modulation coils
E- Phase shifter
N-S, Magnet

Fig. 1V.3

current is used to provide the X-deflection of the C.R.O. display the absorption signal will appear at the centre of the trace if $H = H^{*} = \frac{\omega_o}{\gamma}$, hence the field may be measured from a knowledge of the frequency $\frac{\omega_o}{2\pi}$ of the r.f. input to the bridge.

The absorption signals obtained twice per modulation cycle appear superimposed on the C.R.O. display unless some phase shift occurs in the modulation circuit which then causes the signals to be displaced from one another.

The trace may be calibrated in terms of field strength by simply keeping H_o constant and measuring the frequencies at which the signal appears at the extreme ends of the trace.

In this manner the motion of the N.M.R. signal on the trace due to field fluctuations can be used to estimate the

magnitude of the fluctuations as discussed in section II.5.

The calibrated trace also enables the line-width of the absorption curve to be expressed directly in gauss.

The shape of the absorption curve and the optimum design of the sample coil will be dealt with in a later section.

The amplitude bridge is relatively free from microphonics, since mechanical shocks affect reactive components and thus to a first order alter the phase and not the magnitude of the r.f. voltages, and has proved useful in exploring the field of an electromagnet under constant excitation, provided only very small changes in frequency are required.

The bridge method however is not basically a sensitive detector of the N.M.R. absorption signal and may only be used when the imaginary component of the nuclear susceptibility is inherently large. The audio gain required is high and the limit is set by the degree of residual unbalance of the bridge, the noise introduced by the diodes and the hum pick-up after rectification.

If, during the, an appreciable change of frequency of the r.f. input is required, the following operations must be carried out:-

(i) change the frequency setting of the signal generator

(ii) re-tune the r.f. pre-amplifier

(iii) tune L_1C_1 to resonance at the new frequency

(iv) re-adjust the balance of the bridge.

The necessity for the four independent adjustments enumerated above makes the amplitude bridge unsuitable as a

field discriminator capable of operation over even a small range of frequencies. For such a purpose a single control device is required and attention was therefore directed to a negative resistance type of oscillator and in particular to the transitron oscillating detector described by Knoebel and Hakn.

IV.5 The Transitron N.M.R. Detector

Principle of Operation

In the following treatment of the transitron as a non-linear negative resistance oscillator we consider the problem as a closed loop and apply the notation and methods of servo-mechanism theory. In the transitron proper use is made of the negative resistance characteristics that appear in a pentode valve under certain operating conditions: here we consider the transitron as a two terminal device with negative resistance characteristics appearing between the terminals A and B.

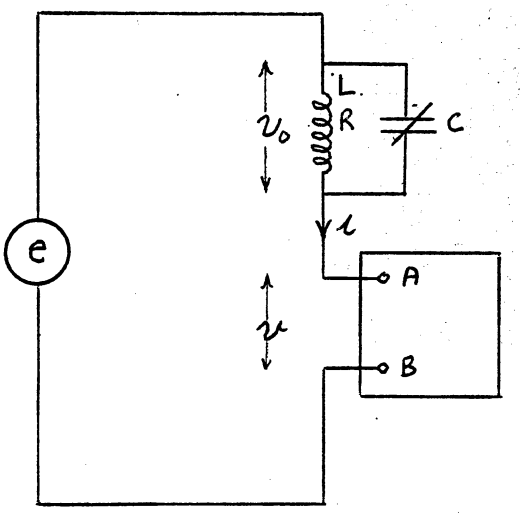

FIG IV·5A

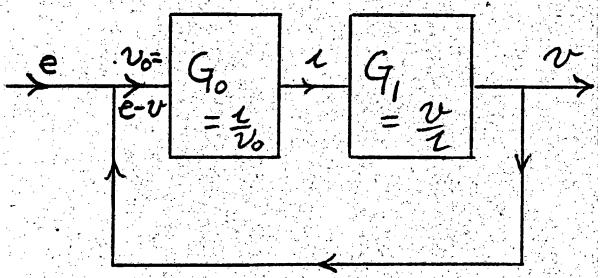

FIG IV·5B

In the circuit of Fig.IV.5A, a tank coil C.L.R. and the transitron are considered connected in series with a hypothetical generator (e.g. noise generator) of e.m.f. 'e'. Fig.IV.5B shows the equivalent closed-loop feedback circuit, from which the loop equation may be directly written as

$$\frac{v}{e} = \frac{G_o G_1}{1 + G_o G_1} \qquad \ldots\ldots\ldots \text{(IV.9)}$$

The loop will be therefore capable of oscillation at a frequency for which

$$1 + G_o G_1 = 0 \qquad \ldots\ldots\ldots \text{(IV.10)}$$

Now the transfer function $G_1 = \frac{i}{v}$ represents the impedance of the transitron between terminals A and B which is assumed to be wholly real. It follows therefore G_o is also real and from its definition ($G_o = \frac{i}{v_o}$) must represent the conductance of the tank circuit. Hence oscillations take place at the frequency which makes the tank circuit conductance real, i.e. at the resonant frequency of the tank circuit.

It is convenient to work in terms of the transitron conductance rather than resistance and since the transitron is a non-linear device its effective conductance under fixed bias conditions is a function of the r.f. voltage, v, across its terminals.

We therefore write

$$G_1 = \frac{1}{G_v}$$

where G_v represents the conductance of the transitron under the operating conditions of bias and amplitude of r.f. oscillation.

The condition for oscillation (equation IV.10) now becomes:-

Negative Conductance Characteristics

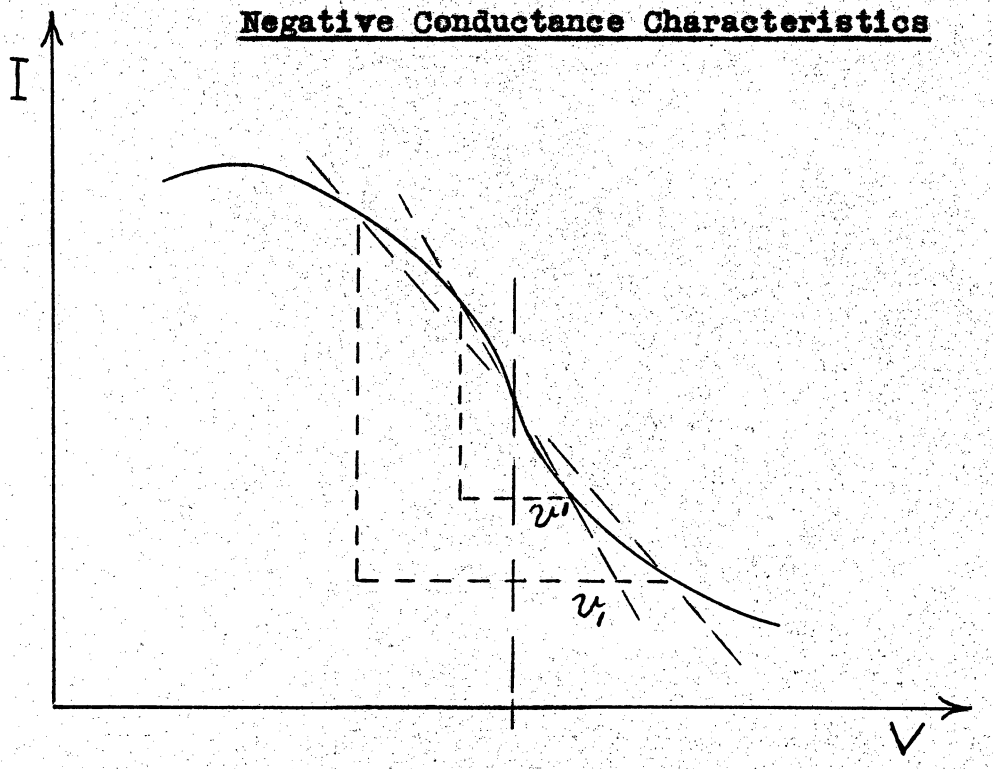

Fig. IV.6

$$1 + \frac{G_{(v)}}{G_o} = 0 \quad \text{or} \quad G_{(v)} = -G_o \qquad \ldots\ldots \text{(IV.11)}$$

i.e. the (negative incremental conductance of the transitron at the operating point must be equal to the conductance of the tank circuit at resonance.

A further condition for stable oscillation is that $\frac{d(G_v)}{dv}$ is negative.

If $\frac{d(G_v)}{dv}$ is positive, the positive feedback in the loop increases with increasing amplitude of the oscillations, which may therefore become self destructive.

On the other hand if $\frac{d(G_v)}{dv}$ is negative and if for some value of v (v' say), $\frac{G_{v'}}{G_o} > 1$, the positive feedback is

greater than unity and oscillations will build up until a value v_1 is reached for which $\frac{G_{(v_1)}}{G_o} \equiv 1$. (Fig. IV.7).

The amplitude of oscillation will not increase further, for if $v'' > v_1$, $\frac{G_{(v'')}}{G_o} < 1$ and the condition for oscillation is not fulfilled.

In considering the effect of N.M.R. on the nuclei of a sample enclosed by the coil of the tuned circuit, it has been shown that the absorption component of the nuclear induction signal gives rise to an effective change in the impedance of the tuned circuit. In terms of conductance we have:-

$$\frac{\delta G_o}{G_o} = -\frac{\delta Z}{Z} = 4\pi\zeta\chi''Q$$

Since for the maintainance of oscillations, $|G_o| = |G_v|$ a change in the conductance of the tuned circuit results in an equal change in the conductance of the transitron and consequently a change in the level, δv, of the r.f. voltage across the transitron terminals.

For small changes we may write

$$\delta G_{(v)} = \frac{dG_{(v)}}{dv}\ \delta v$$

or

$$\delta v = \frac{\delta G_{(v)}}{\frac{dG_{(v)}}{dv}} = \frac{\delta G_o}{\frac{dG_v}{dv}}$$

whence

$$\delta v = \frac{G_o \cdot 4\pi\zeta\chi''Q}{\frac{dG_v}{dv}} \qquad \ldots\ldots\ldots \text{(IV.12)}$$

Comparing the above with equation (IV.7) we note that there

is an effective magnification of the N.M.R. absorption signal if $\frac{G_o}{v\left(\frac{dG_{(v)}}{dv}\right)} > 1$. Although at the inflection point of the I-V characteristic curve $\frac{dG_v}{dv} = \frac{d^2I}{dV^2} = 0$, the above expressions are only approximately true since δv is finite; nevertheless a greater magnification of the N.M.R. signal is obtained if the operating point coincides with the inflection point and the amplitude of the r.f. voltage is kept small.

IV.6 Transitron Design and Operation

Fig. IV.7 shows the static characteristics of a typical 6AS6 pentode and illustrates the existence of a negative resistance that appears between the r.f. common screen and suppressor grid terminal and ground. The 6AS6 tubes are chosen as being particularly suitable for transitron operation and from a given batch, those tubes which have the best characteristics are selected.

Fig. IV.8 shows the circuit details of the transitron oscillator which is essentially the same as that described by Knoebel and Hahn. The tuned circuit, consisting of the variable condenser C and inductance L which is wound on the sample vial, is connected between grids 2 and 3 and ground. The r.f. chokes RFC_1 and RFC_3 isolate the r.f. oscillations from the plate and filament respectively while RFC_2 prevents the grid 2 bias supply from shunting the tuned circuit. De-coupling filters are provided where appropriate.

The variations of amplitude of the r.f. oscillations

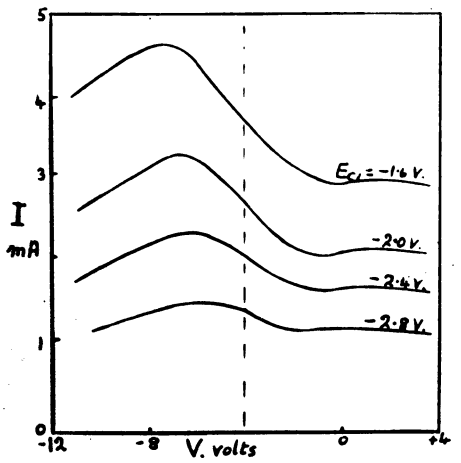

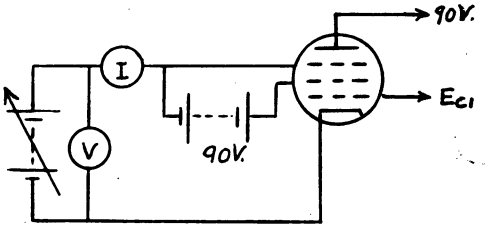

Fig IV·7

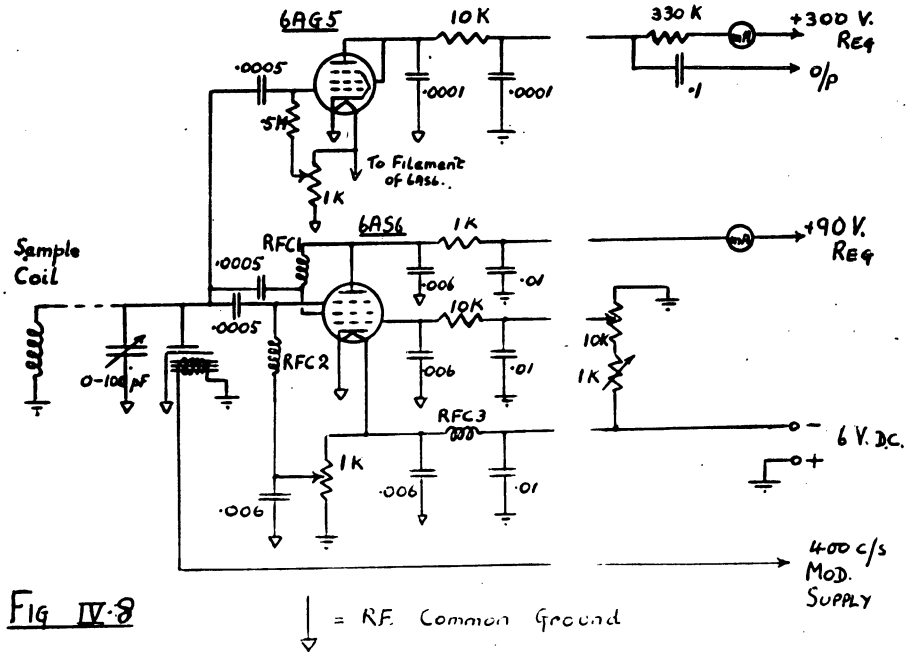

Fig IV·8

= R.F. Common Ground

that occur at resonance, are detected by the 6AG5 which is connected as a triode and biased for anode bend detection, and the detected output is passed on to an audio-amplifier.

In operation, grid 1 bias, which controls the plate current is adjusted until oscillations are just maintained, while grid 2 bias is adjusted so that the operating point coincides with the inflection point of the $I_{g_2}-V_{g_2}$ characteristics The existence of oscillations may be detected by the presence of noise on the monitoring C.R.O. and by an increase in the detector plate current.

In construction, attention was paid to the normal techniques employed at radio frequencies such as common r.f. ground, shielding etc. and no serious difficulty was encountered apart from mains 50 c/s pick up which was considerably reduced by paying further attention to the earthing of the apparatus as a whole.

A very important consideration is the Q factor of the sample coil. It has been pointed out above, that a condition for the existence of stable oscillation is that at some point on the $I_{g_2}-V_{g_2}$ characteristic $G_v > G_o$ i.e. the impedance of the tuned circuit at resonance (QWL) must be slightly greater than the negative resistance of the transitron at the operating point. Since the latter is determined by the transitron characteristics, this implies that the resonant impedance of the tuned circuit and hence the Q must exceed certain minimum values. In addition, the presence of Q in the numerator of equation IV.10 requires that for an optimum signal, Q must be as large as possible.

Thus the damping effect of the probe on the sample coil must be kept to a mimimum. This can be effected by ensuring that the inside diameter of the probe exceeds that of the coil by a factor of 1.5 (preferably 2) and by avoiding the use of lossy dielectric in the supports of the coil and of the axial conductor which runs the length of the probe.

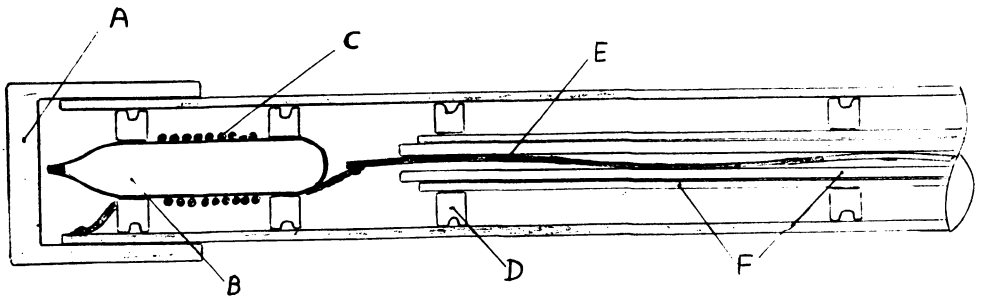

A- Shield cap
B- Sample vial
C- Sample coil
D- Rubber grommets
E- Axial conductor
F- Glass tubing

Fig. IV.9

Fig. IV.9 shows the details of the construction of such a probe, in which in order to reduce microphonics, the axial conductor is supported in a thick-walled glass tube, which is itself supported in the probe by means of rubber grommetts. The sample of ferric nitrate solution is contained in a vial made from thin-walled glass tubing 0.8cm outside diameter. The coil contains 8 turns of 26 gauge enamelled wire wound tightly on the vial which is also supported by rubber grommetts.

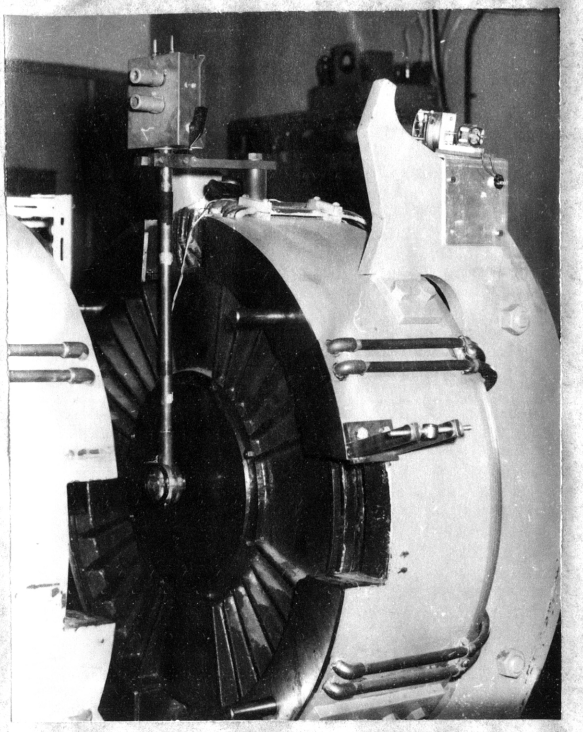

Fig. IV.10

Field modulated Transitron shown in position in the gap of the U.N.S.W. magnet.

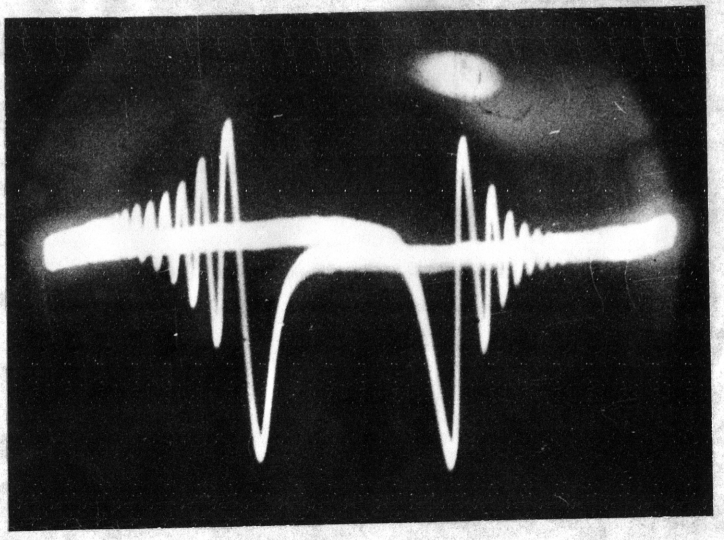

Fig. IV.11

Proton absorption signal obtained from a Transitron detector employing a wide sweep field modulation.

(Line width $\doteq$ 0.3 gauss)

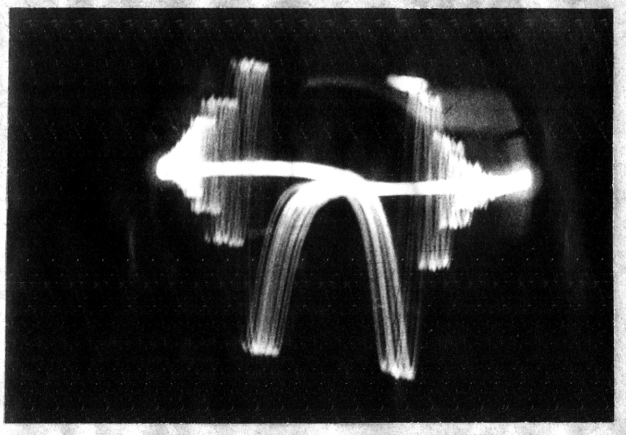

Fig. IV.12

Oscillogram of absorption signal taken with a 0.5 sec. exposure showing the effects of the generator ripple on the magnet field.

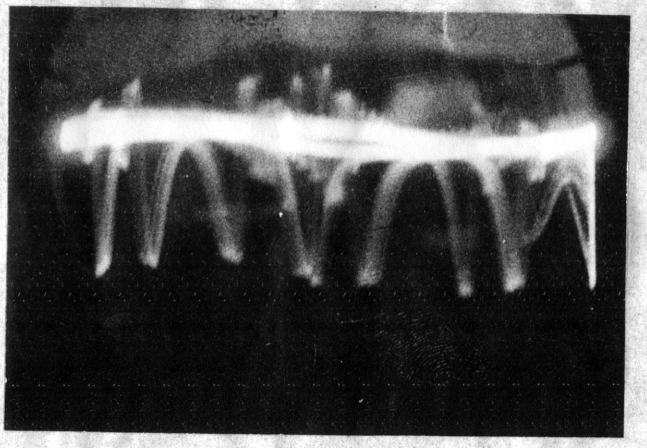

Fig. IV.13

Multi-exposure oscillogram taken at 5 sec. intervals of the slow drift and random fluctuations of the magnet field.

One end of the coil is connected to the stout axial conductor while the other end is soldered directly to the probe itself.

A transitron unit employing field modulation and an oscillogram of the absorption singal from a proton sample (ferric nitrate solution) are shown in Figures IV.II, in which the signals are observed to be separated due to a phase shift in the modulation circuit.

This transitron unit has been used in an exactly similar manner to that of the amplitude bridge, and has been used as a field discriminator (Sect. V) for stabilisation purposes. For the latter purpose however it is necessary that the field discriminator should not itself interfere with other apparatus in the magnetic field, and frequency modulation of the transitron is preferred to modulation of the magnetic field.

Modulation of the transitron frequency has been effected in a simple manner by the use of a variable capacitor which takes the form of a vibrating reed and a fixed plate, and is connected in parallel across the tuning condenser of the tank circuit. A coil energised from the modulation supply is wound on a laminated U-shape core, and the reed, in the form of a piece of thin spring steel, $1\frac{1}{2}$" x $\frac{3}{8}$", is clamped at one end to an arm of the core and extends across the gap of the U-core. The insulated "fixed" plate is mounted parallel to the reed and in such a manner that the distance of separation may be made any desired amount. The whole unit encompasses a volume $1\frac{1}{2}$" x 2" x $2\frac{1}{2}$".

In order to obtain sufficient amplitude of vibration of the reed to produce the 0.1% index of frequency modulation rwquired when searching for the N.M.R. signal, it has been found necessary to tune the natural frequency of the reed to the modulation frequency. This is done by filing the reed in an appropriate manner so as to reduce its rigidity and thus its natural frequency of vibration.

In fitting the vibrating reed modulator into the shield box of the transitron unit, heavy brass shielding was required to reduce direct pick up at the modulating frequency by the transitron itself, and to damp down microphonic pick up at this frequency.

V - N.M.R. FIELD DISCRIMINATOR

V.1 Theory

The N.M.R. absorption signal has a finite linewidth since all nuclei in the sample are not subject to the same magnetic field. In the case of a liquid sample (as used in the discriminator) the rapid brownian motion effectively destroys the local field to which a given nucleus is subjected due to the magnetic moment of its neighbours and the natural linewidth is consequently very small ($\sim 10^{-4}$ gauss). The observed linewidth in then entirely due to the unhomogeneity of the magnet field over the sample valume.

The presence of a field gradient in the magnetic field may give rise to a beat effect or "wiggles". This can be seen in the oscillogram of Fig. IV.11 where the modulation sweep is approximately 20 linewidths.

However as the field discriminator operates with a modulation less than the linewidth this effect does not arise.

In cases where the inhomogeneity is due to the magnet, increasing the sample volume will not increase the peak-height of the signal, but only increases the linewidth.

On the other hand, decreasing the sample volume by decreasing the coil dimensions lowers the Q of the coil, which in turn reduced the signal output. A compromise between these conflicting requirements has to be sought, and for operation over a fixed frequency range (i.e. for a given coil inductance) the optimum coil dimensions may be found by a trial and error method.

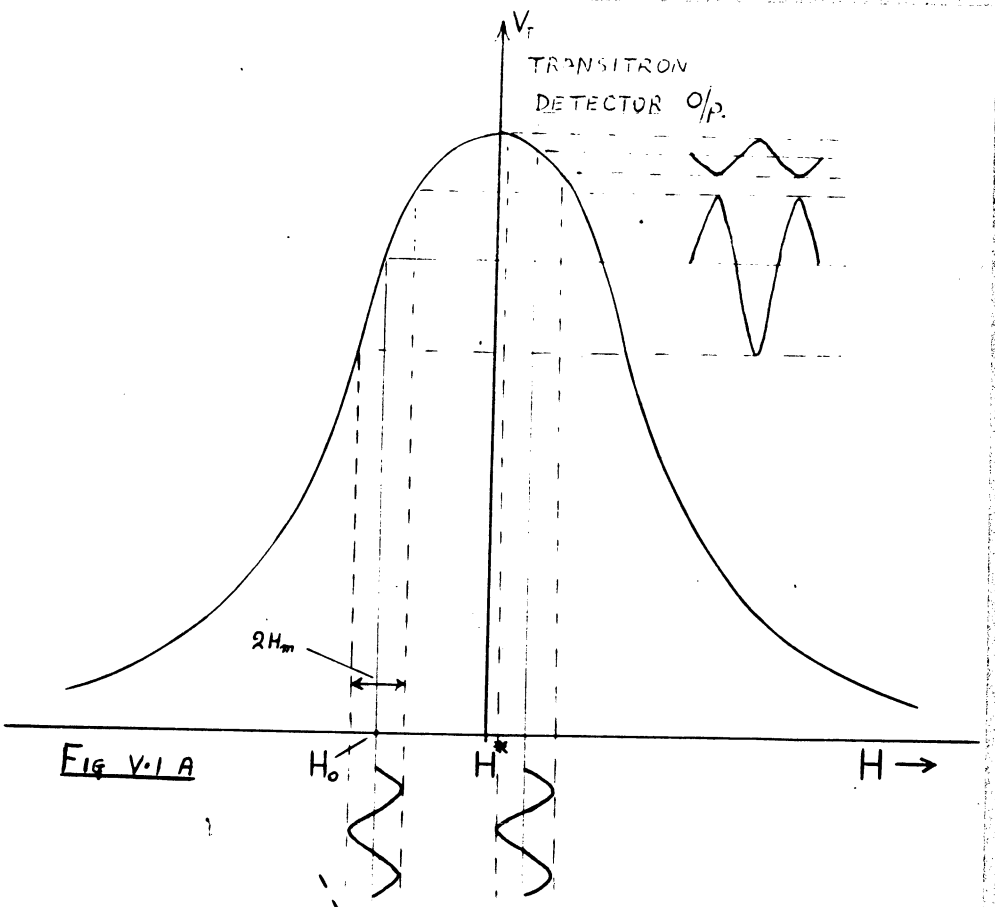

FIG V·1 A

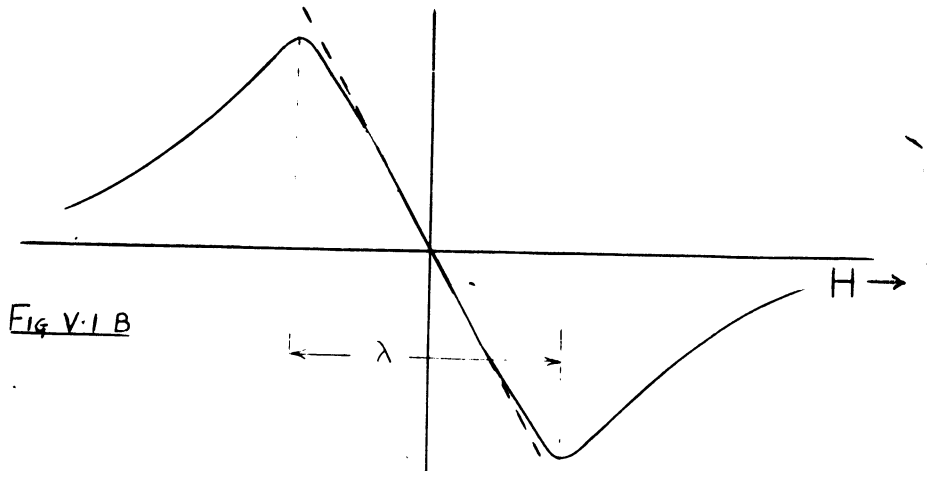

FIG V·1 B

The output of a N.M.R. absorption detector as the magnetic field is swept through the resonant field H^* is shown in idealised form in Fig. V.1A.

If we now consider the magnetic field to have a steady value H_o, and the sample to be subjected to a small modulating field $H_m \sin pt$, where H_m is a small fraction of the linewidth , the r.f. amplitude will be modulated with a fundamental frequency equal to the frequency of the field modulation $\frac{p}{2\pi}$ and the detector output will be a voltage which again has a fundamental frequency of $\frac{p}{2\pi}$.

From a consideration of the diagram (Fig. V.1A), it will be seen that the detector output will have a fundamental whose magnitude depends on the departure of the steady value of the magnetic field H_o from the resonant value H^* i.e. upon $|H^* - H_o|$, and whose phase relative to the modulating field $H_m \sin pt$ is either 0 or π depending on whether $(H^* - H_o)$ is positive or negative.

Furthermore, if the N.M.R. detector output is fed into a phase sensitive rectifier a D.C. voltage may be obtained which is either positive or negative depending upon the above phase relations and which may be used to control the magnet field in such a manner that $|H^* - H_o| \longrightarrow 0$.

For values of H_m very small compared with the linewidth of the N.M.R. absorption signals , the output of the phase sensitive rectifier is as shown in Fig. V.1B and is essentially proportional to the derivative of the absorption curve of Fig. V.1A.

The output of an ideal field discriminator (dotted line curve of Fig, V.1B) is proportional to $(H^* - H_o)$ for all values of $(H^* - H_o)$.

The N.M.R. field discriminator falls short of this ideal and an approximately proportional output is only obtained if $|H^* - H_o| < \frac{\lambda}{2}$.

If through any cause, a change occurs which brings H_o beyond the inflection points of Fig. V.1A, i.e. if $|H^* - H_o| > \frac{\lambda}{2}$, the output of the phase sensitive rectifier will vanish, and the discriminator will cease to function altogether.

In practice, the modulating field cannot be made too small, or else the N.M.R. detector output will be entirely marked by noise. With a finite modulation amplitude, there will exist in the N.M.R. detector output harmonics, particularly the second harmonic, the magnitude of which will depend on the amplitude of the field modulation, and on the curvature of the absorption signal at the operating point.

The presence of second harmonic does not affect the operation of the phase sensitive rectifier and it has been found that for optimum performance of the stabilising loops, it is necessary to make the modulation sweep approximately 1/3 of the linewidth. The presence of second harmonic is then most noticeable.

At an early stage in the development it was feared that noise and second harmonic in the N.M.R. detector output might affect the operation of the phase sensitive rectifier and subsequent stabilising feed-back loop. A narrow band

stage, which could be switched in or out as desired, was therefore incorporated in the audio amplifier. With narrow band amplification, noise and second harmonic are removed from the input to the phase sensitive rectifier, but it was subsequently found that the narrow was unnecessary and the operation of the feedback loop as a whole was, if anything, improved by not using it.

In the above discussion it has been assumed that field modulation was employed. However, because of the linear relationship between resonant field and frequency, it is possible to maintain a constant field and to modulate the r.f. The above relationships then remain valid if we write

$H_m = m_f \cdot \frac{\omega_o}{\gamma} = m_f \cdot H^*$, where m_f is the modulation index of the frequency modulated r.f.

V.2 Design and Operation of the Field Discriminator

Fig. V.2 gives a block diagram of the field discriminator used as an integral part of a stabilising feed-back system.

A transitron oscillator, which is either frequency or field modulated (both have been employed), is used to detect the N.M.R. absorption signal in a water sample.

A 400 c/s. generator which consists essentially of a Wien Bridge oscillator locked to the eighth harmonic of the mains frequency, provides a reference signal for the phase sensitive rectifier and, after a stage of power amplification, the modulation source (frequency or field) for the transitron.

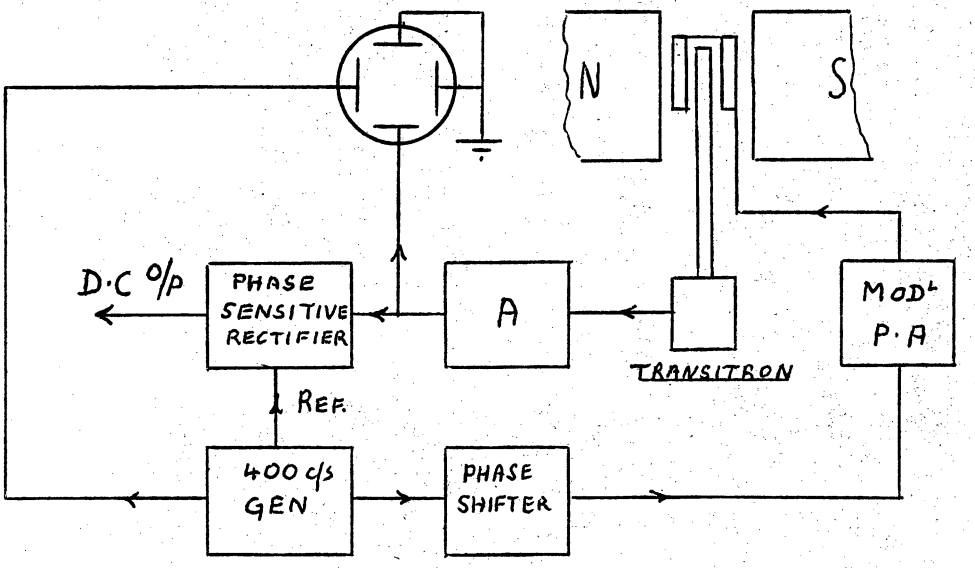

FIG V·2

The 400 c/s generator output to the power amplifier is capable of being shifted in phase so that the reference signal and the detected transitron signal appear at their respective inputs to the phase sensitive rectifier with the correct phase relationship

400 c/s was chosen as the modulation frequency as being sufficiently removed from the mains frequency so that when used in conjunction with the narrow-band amplifier, any 50 c/s hum pick up in the output of the transitron would not be passed on to the phase sensitive rectifier. This precaution ultimately proved unnecessary and as has been previously mentioned the discriminator is used with the narrow-band stage shorted out.

The transitron signal, after amplification is displayed on a CRO: when searching for resonance, a wide modulation sweep ($>10\lambda$) is used and the voltage applied to the X-deflection plates is derived from the modulation source.

(In the case of field modulation, the modulation

supply, for searching purposes only, was obtained from the 50 c/s mains through a 12V transformer, as insufficient drive for the Helmholtz modulation coils could be obtained from the power amplifier).

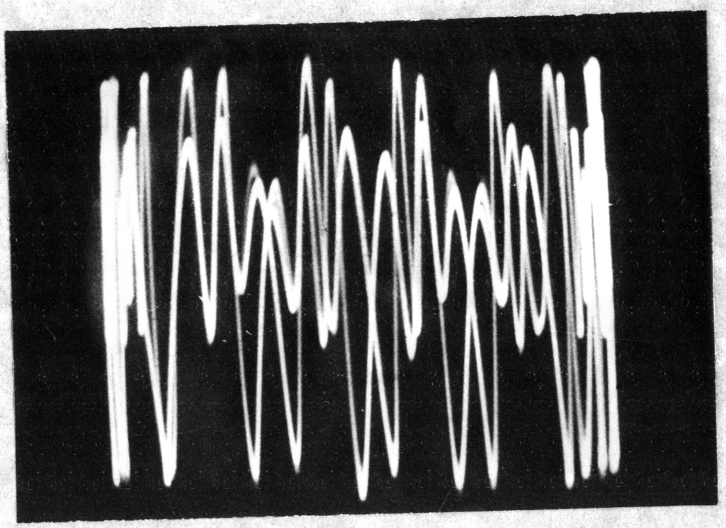

Fig. V.3

Oscillogram of the output of a frequency modulated Transitron detector. The second harmonic predominates indicating that the magnet field is very close to the resonant value H.
(The X-deflection is 50 c/s, sinoidal.)

When modulating at 400 c/s within the line width, the X-deflection was obtained from a 50 c/s mains source, since the Lissajous figure thus obtained was the more easily interpreted. This is illustrated in the oscillograms of the amplified output of a frequency modulated transitron employing a modulation sweep of approximately 1/3rd of the line width. (Fig. V.3). If $H_o = H^*$ the transitron output is essentially all second

harmonic of the modulation frequency, and the corresponding output of the phase sensitive rectifier is zero.

When $0 < |H_o - H| < \frac{\lambda}{2}$, the transitron output contains components at the fundamental and second harmonic of the modulation frequency.

Details of the 400 c/s generator, the audio amplifier and modulation supply power amplifier are given in the appendix.

The phase sensitive rectifier is however an integral com component of the field discriminator and a brief description of its operation will be given with reference to the circuit diagram of Fig. V.4.

The two 6J6 triodes are connected in parallel opposition as shown and reference signals from the 400 c/s generator, equal in magnitude and in phase, are applied to the grids of the tubes, which operate under Class C conditions and are provided with grid leak bias.

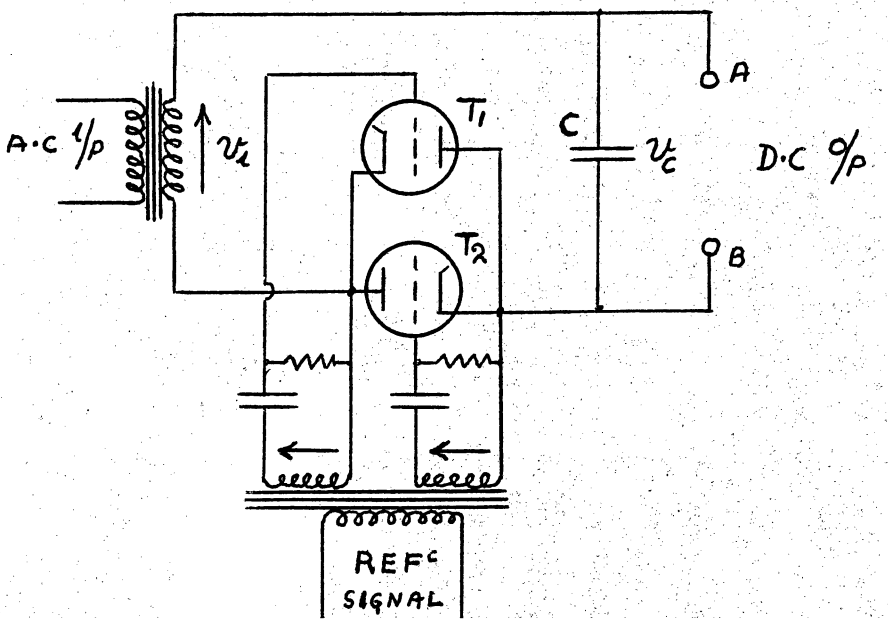

If the input from the audio amplifier has phase with respect to the reference signals as shown by the arrows in the diagram, then tube T_2 will remain non-conducting while T_1 conducts during the positive half-cycle and the condenser C will charge up (the terminal A becoming positive) at a rate determined by the values of C and the effective resistance of the tube during the conducting period, i.e. the charging time constant is small. During the negative half-cycle neither valve conducts and the condenser C maintains its charge except for a very small leakage determined by C and the load resistance. After a few charging cycles, the voltage across C, (V_C) becomes equal almost to the peak input voltage (V_i) and the charging current becomes very small, being just sufficient to make up for the leakage during the non-conducting cycle. Should the input voltage V_i increase in magnitude current will flow during the conducting half-cycle of T_1 so as to make V_C equal almost to V_i.

If V_i decreases in magnitude, ($V_i - V_C$) becomes negative, T_1 ceases to conduct while T_2 now conducts and the condenser C discharges until ($V_i \rightarrow V_C$) $\rightarrow 0$.

If the phase of the input voltage is reversed with respect to the reference voltages, the tubes T_1 and T_2 exchange roles and the condenser C charges up so that terminal B now becomes positive.

The output of the phase sentive rectifier is essentially linear with input up to approximately 60V D.C. output. The gain of the audio amplifier is therefore adjusted in normal

operation, so that when the transitron output is a maximum (i.e. when H_0 corresponds to either the inflection points of the absorption curve) then the phase sensitive rectifier output is 60V. D.C.

A particular feature of this type of phase sensitive rectifier, in addition to its simplicity and short time constant ($\sim$0.01 sec), is the fact that the output is isolated from earth and the connection to the subsequent feed-back loop is thereby simplified.

V.3 Experimental Difficulties

In the early attempts to obtain a correction signal and to apply it to a feed-back correction loop, a field modulated transitron was used as a field discriminator, while an amplitude bridge N.M.R. detector employing a wide sweep field modulation was used as a field monitor i.e. to determine the actual behaviour of the magnetic field.

As the field was brought up to the resonant value, a correction signal was generated that bore no resemblance in magnitude or sign to what was expected. It was some time before the obvious solution to this anomolous behaviour was realised, namely, that the sample was being subjected to a stray modulation field from the modulation coils of the amplitude bridge monitor.

It was therefore decided to convert the transitron to a frequency modulated version for use as a field monitor, and to construct a second transitron for use as a field discriminator.

Further attempts to obtain a useful correction signal

were however still frustrated. The anomolous behaviour still persisted as though some spurious modulation of small amplitude were present.

After a prolonged and systematic search the trouble was traced to a frequency modulation of the r.f. of the discriminator transitron at a rate of 100 c/s.

This was caused by microphonic vibration of the transitron and was due to the fact that transitron was being supported in a retort stand standing on the same bench as other electronic apparatus.

When the transitron was mounted in a rigid clamp firmly attached to the magnet yoke, this trouble disappeared.

VI. - PERFORMANCE OF THE COMPLETE STABILISING SYSTEM

VI.1 Slow Drift

The field discriminator provides an error signal which can be used to correct for slow drift in the magnetic field. This error signal which is proportional to $(H - H_o)$ is applied to the grid of the power amplifier of the generator field circuit.

As a basis for design it was assumed that the maximum slow drift for which it would be necessary to correct would amount to 10% of the total magnet field. Since the maximum

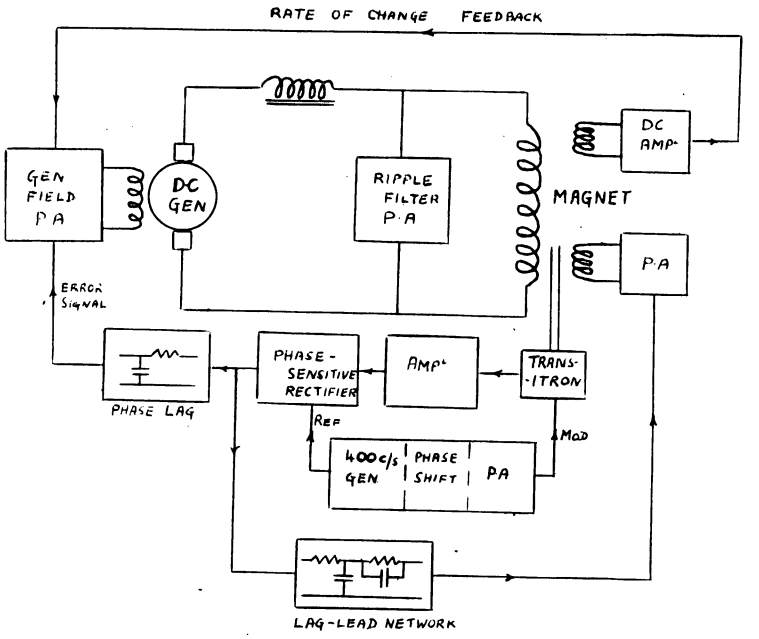

FIG VI·1

error that can be tolerated is half the linewidth of the N.M.R. absorption signal (say 0.1 gauss) the feedback loop gain required, for a magnet field of 10^4 gauss, would be

$$\frac{10^4 \text{ gauss} \times 10\%}{0.1 \text{ gauss}} = 10^4$$

With such a high gain, the loop is unstable. (Oscillations commence when the loop gain is of the order of 10^2).

It is necessary therefore, to maintain the D.C. gain at 10^4, yet reduce its value to less than unity at frequencies for which the phase shift around the loop is 180°.

This may be realised to some extent by the use of a passive phase-lag network which takes the form of a simple R.C. combination having a large time constant, and which is inserted into the loop immediately following the phase sensitive rectifier. (Fig. VI.1).

With a phase lag network having a time constant of 50 sec., the D.C. gain may be increased to 10^4 and the system remains conditionally stable; that is, after a system dusturbance or a change in reference input (i.e. change of transitron oscillator frequency) the field performs damped oscillation of small amplitude.

However with the introduction of a further element of large time constant into the loop, if the disturbance or change in reference occurs at too fast a rate, the amplitude of the transient oscillations may be such that the instantaneous error, $(H^* - H_o)$, exceeds the half linewidth so that the N.M.R. field discriminator ceases to operate.

The effect of this oscillation has been reduced and the stability improved by the addition of a subsidiary feedback loop which incorporates a phase lag-lead network and provides an additional correction in the critical frequency range. The error signal from the output of the phase sensitive rectifier is fed through the lag-lead network onto the grid of a small power amplifier which contains a subsidiary (H.Z) magnet excitation coil as plate load. The values of circuit components in the lag-lead network, which gave the optimum performance, were determined empirically.

VI.2 Scanning the Magnet Field

For certain purposes it may be necessary to change the magnet field by a few percent, in order that it may be brought

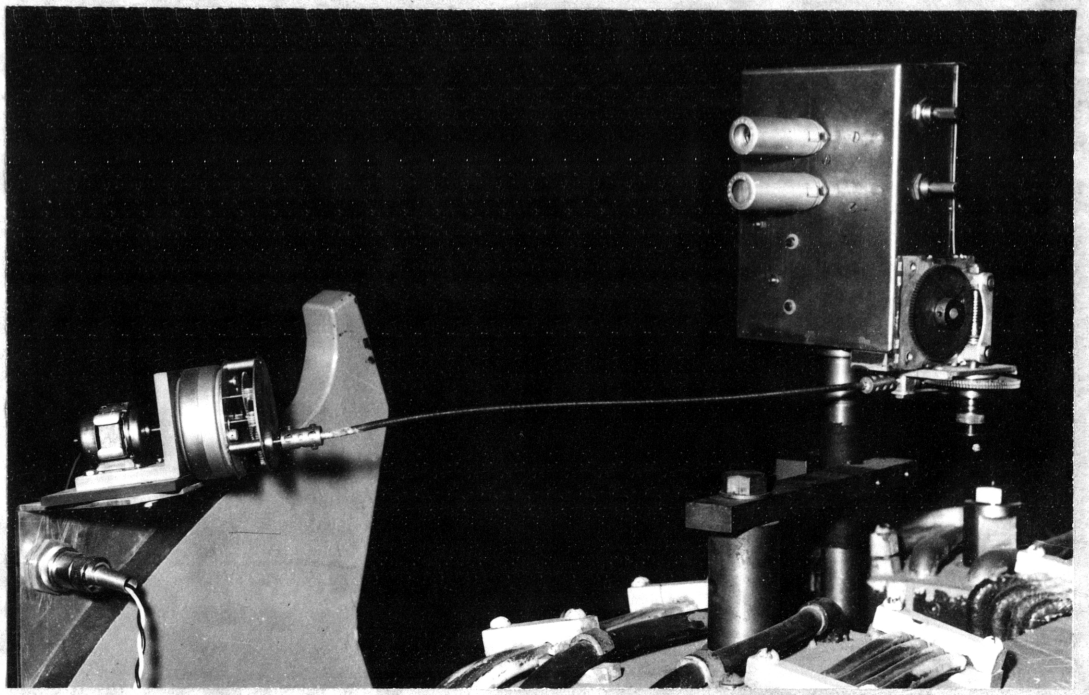

FIG. VI·2

to some desired exact value, the field being kept stabilised while the change is being made.

This has been accomplished by changing the reference i.e. by slowly changing the transitron frequency by adjustment of the tuning condenser.

A small reversible electric motor drives a reduction set of gears (from an electric clock) which in turn is connected by means of a flexible cable to a worm and wheel reduction gear mounted on the transitron shield box. (See Fig. VI.2). This gear is connected through a friction clamp to a second worm gear which is attached to the shaft of the transitron tuning condenser.

When the friction clamp is unscrewed, the motor ceases to drive the second worm gear and adjustments may be made manually by means of a knob attached to the shaft of the second worm.

The motor is supplied from a 6 volt accumulator and its speed may be varied by means of a series resistor.

VI.3 Performance

Fig. VI.3 shows portion of the record of the voltage occurring across the magnet terminals under various conditions:-

AB - no feedback loop in operation

BC - ripple filter and rate-of-change subsidiary feedback in operation

CD - complete stabilising system in operation.

In considering the latter portion (CD) it must be

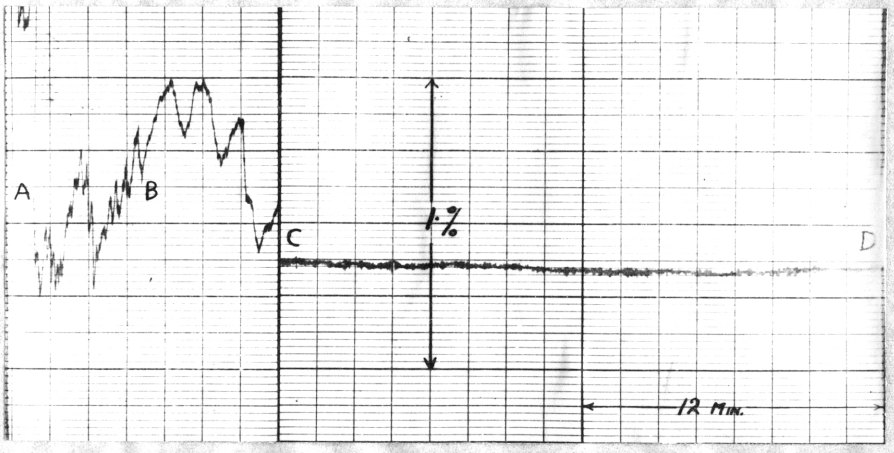

FIG VI·3

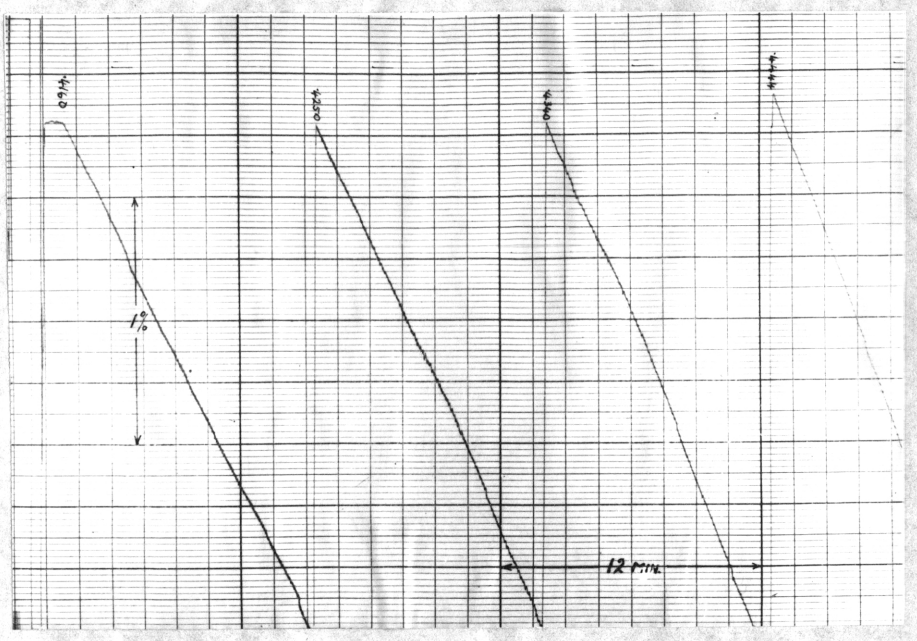

FIG VI·4

remembered that, the voltage across the magnet terminals may vary slightly, yet the magnetic field remains constant. Since the N.M.R. feedback loop remained in operation it follows that the greatest deviation of the field H_o from the resonant value H^* was less than half the linewidth of the N.M.R. absorption signal ($\sim$.15 gauss).

Thus in a field of approximately 7,000 gauss, we may say that the field was held constant to within 2 parts in 10^5.

In the record of Fig. VI.4, the frequency of oscillation of the transitron was varied at a constant slow rate. Since $|H^* - H_o| \leq \frac{\lambda}{2}$, it follows that the magnet field changed at a similar rate.

The maximum change that took place before the discriminator failed to operate, was 9.5% and occurred at a rate of 20 gauss/min.

Since as far as the operation of the discriminator is concerned, changes of frequency and of magnetic field have the same effects, we may assume that, if the frequency had been kept constant, and a disturbance had been applied to the system, which, in the absence of any stabilisation loop, would have produced the same change in field as that described above, then with the stabilisation loop in operation the field would have been maintained at a constant value.

In stating that, if the transitron frequency is not deliberately changed, the field remains constant to 2 parts in 10^5, it is assumed that the transitron frequency is itself constant.

A check on the stability of the frequency of the transitron oscillator has been made, by loosely coupling a signal from the transitron to a crystal controlled master oscillator, the resultant beat frequency signal being then measured by a rate meter.

After an initial warm-up period during which the frequency change was .01%, it was found that over a period of 6 hours the transitron frequency remained constant to within 300 c/s in 30 Mc/s i.e. a stability of 1 part in 10^5.

VI.4 Conclusions and Comments

The stabilising system described above will hold the field of the University of New South Wales magnet constant to within 2 parts in 10^5 and will accommodate slow changes of excitation of up to 9.5% in a field of 7,000 gauss.

The degree of stabilisation is limited by the line-width of the N.M.R. absorption signal obtained from the given sample, and an increase in the stability may only be accomplished by a further improvement of the homogeneity of the field of the magnet. Assuming this to be attained, a number of problems would then present themselves.

Firstly, the present arrangements for smoothing the magnetic field may prove unsatisfactory i.e. the residual fluctuations which are negligible compared with an absorption signal linewidth of 0.3 gauss may not prove insignificant with a linewidth of, say, 0.01 gauss.

Secondly, with the increase of loop gain required to

produce a field stability of 1 in 10^6, the feedback loop through the D.C. generator may prove unstable.

Thirdly, in order to achieve a field stability of 1 in 10^6, the transitron oscillator must be capable of a frequency stability of the same order.

It therefore appears that little further increase in stability can be obtained with the present system and that to attain any marked improvement a completely new approach may be required. One method which suggests itself is to employ power transistors which have recently become commercially available to provide a stabilised current supply for a constant excitation and to use a crystal stabilised N.M.R. discriminator feeding into the auxiliary magnet coils in order to provide correction for the changes in magnet field that occur due to thermal changes in magnet geometry and permeability.

A C K N O W L E D G E M E N T S

The author wishes to thank his supervisor Mr. L.O. Bowen for helpful advice and discussions at all stages of the development of this project. He also acknowledges the assistance given by Mr. E.Laisk, Electronics Workshop and Mr. R.Menere, Mechanical Workshop.

REFERENCES

N.M.R. Theory

Block, Hanscen and Pakard — Phys.Rev.70,460(1946)

Bloembergen, Purcell and Pound — Phys.Rev.73,679(1948)

N.M.R. Detectors

Thomas and Huntoon — Rev.Sci.Inst.20,516 (1949)

Knsebel and Hahn — Rev.Sci.Inst.22,704 (1951)

M.E. Packard — Rev.Sci.Inst.19,435 (1948)

Stabilisation of Magnetic Fields

Wolff and Freedman — Rev.Sci.Inst.22,736 (1951)

Sommers, Weiss and Halpem — Rev.Sci.Inst.20,244 (1949)

Sommers,Weiss and Halpem — Rev.Sci.Inst.22,612 (1949)

M.E.Packard — Rev.Sci.Inst.19,435 (1948)

H.A.Thomas — Electronics 25,114 (1952)

University of New South Wales Magnet Design and Performance

L.O.Bowen — Jnl.Sci.Inst.34,265 (1951)

Textbooks

Brown and Campbell — Principles of Servomechanism Wiley 1948

Bruns and Saunders — Analysis of Feedback Control Systems, McGraw-Hill 1955

Valley and Wallman — Vacuum Tube Amplifiers M.I.T. Radiation Lab. Series No.18 McGraw-Hill 1948

APPENDIX A

Effects of Eddy Currents on Magnet Response

As a basis for this simple model we consider the magnet as a transformer with the circulating eddy currents in the core forming an equivalent to a short-circuited secondary.

The main excitation coils of the magnet which form the primary are assumed, in the absence of eddy currents, to have an inductance, L_c and resistance R_r. The eddy current secondary is assumed to have an effective inductance L_e and effective resistance R_e.

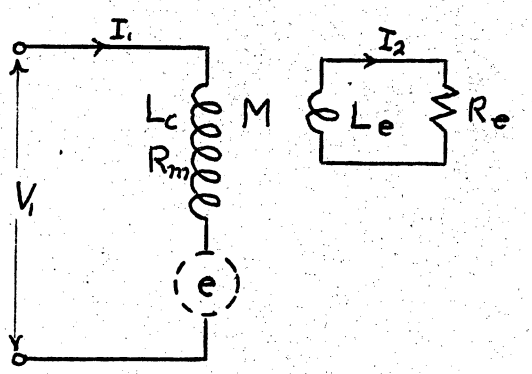

FIG A·1

Following the usual treatment of coupled circuits the effective primary impedance is

$$Z' = \frac{V_1}{I_1} = Z_1 + \frac{\omega^2 M^2}{Z_2}$$

where M is the coefficient of mutual inductance between primary and secondary windings

and $Z_1 = R_m + j\omega L_c$, $Z_2 = R_e + j\omega L_e$

Now the coefficient of coupling, k, is defined by

$$k = \sqrt{\frac{M}{L_c L_e}}$$

Hence

$$Z' = \frac{R_m R_e - \omega^2 (L_c L_e - k^2 L_c L_e) + j\omega (R_e L_c + R_m L_e)}{R_e + j\omega L_e}$$

$$= R_m \cdot \frac{1 - \omega^2 \tau_c \tau_e (1 - k^2) + j\omega (\tau_c + \tau_e)}{1 + j\omega \tau_e}$$

where

$$\tau_c = \frac{L_c}{R_m} \quad \text{and} \quad \tau_e = \frac{L_c}{R_e}$$

The transfer function for a voltage applied to the magnet terminals is given by

$$G_1 = \frac{I_1}{V_1} = \frac{1}{Z'},$$

Hence

$$G_1 = \frac{1}{R_m} \cdot \frac{1 + j\omega \tau_e}{1 - \omega^2 \tau_e \tau_e (1 - k^2) + j\omega (\tau_e + \tau_c)} \quad \ldots (1)$$

If, we may assume that the primary and eddy current secondary are closely coupled i.e. if $k \longrightarrow 1$.

Then

$$G_1 = \frac{1}{R_m} \cdot \frac{1 + j\omega \tau_e}{1 + j\omega (\tau_e + \tau_c)} \quad \ldots\ldots\ldots (2)$$

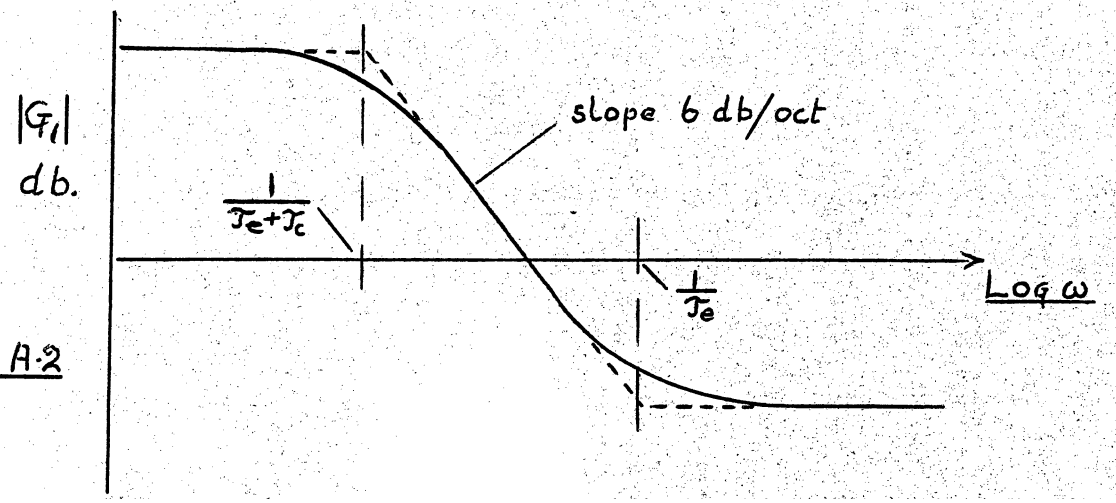

FIG A·2

This function is illustrated in Fig. A.2 and may be compared with the experimental results of Fig.II.5. The dotted line shows the asymptotic approximation and illustrates the significance of the "break" frequencies

$$\frac{1}{\tau_c + \tau_e} \quad \text{and} \quad \frac{1}{\tau_e}.$$

It will be observed that for frequencies for which $\omega \tau_e \gg 1$

$$Z' = \frac{1}{G_1} = R_m \cdot \frac{\tau_c + \tau_e}{\tau_e}$$

i.e. the impedance of the magnet is purely resistive.

The field in the gap of the magnet is the sum of the fields due to the excitation current and eddy currents. We therefore write

$$H = C_1 I_1 + C_2 I_2$$

where C_1 and C_2 are constants depending on the magnet geometry, number of turns, etc.

Now, for two coils having N_1 and N_2 turns respectively wound on the same toroidal core

$$\frac{C_1}{C_2} = \frac{N_1}{N_2} = n \text{ (say)} \quad \text{and} \quad \frac{L_1}{L_2} = \frac{N_1^2}{N_2^2} = n^2.$$

We assume that these relationships remain sufficiently accurate for the magnet when one of the coils is the "eddy current" secondary. Thus

$$M = k\sqrt{L_c L_e} = k\sqrt{(n^2 L_e)\, L_e} = knL_e$$

and since $I_2 = -\frac{j\omega M}{Z_2} I_1$

we obtain

$$H = C_1 I_1 - C_2 \frac{j\omega knL_e}{R_e + j\omega L_e}$$

Hence for the transfer function G_2 for the field produced by a current flowing in the primary is given by

$$G_2 = \frac{H}{I_1} = C_1 \cdot \frac{1 + j\omega \tau_e(1 - k)}{1 + j\omega \quad _e}$$

for perfect coupling this simplifies to

$$G_2 = C_1 \cdot \frac{1}{1 + j\omega \tau_e} \qquad \ldots\ldots (2)$$

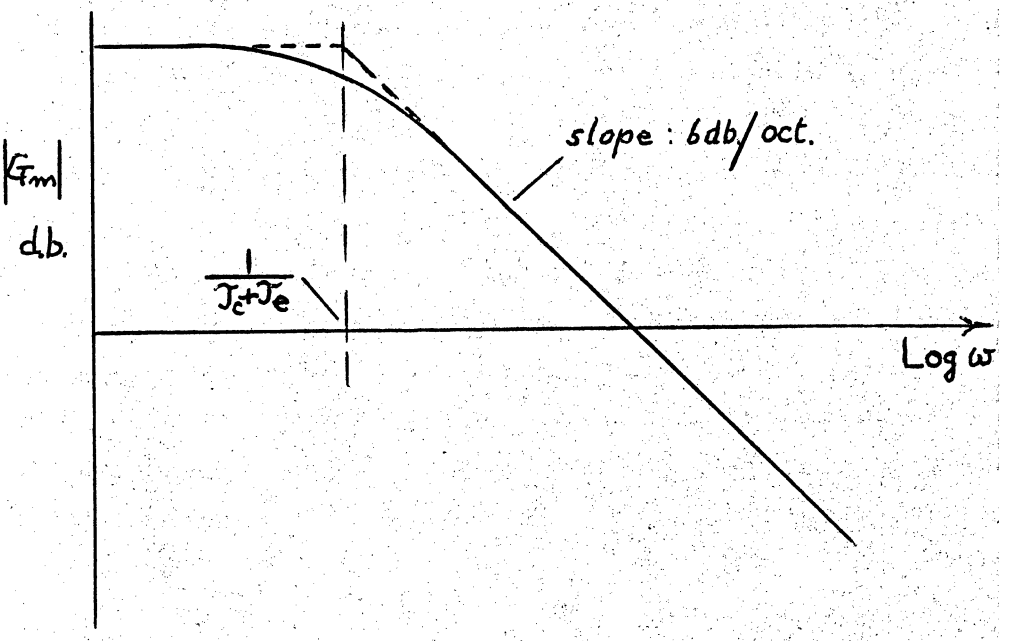

FIG A·3

For the magnet as a whole, the transfer function for a voltage applied at the magnet terminals is defined as

$$G_m = \frac{H}{V_1} = \frac{H}{I_1} \cdot \frac{I_1}{V_1}$$
$$= G_2 \cdot G_1$$

Thus

$$G_m = \frac{1}{R_1} \cdot \frac{1 + j\omega \tau_e}{1 + j\omega(\tau_c + \tau_e)} \cdot C_1 \frac{1}{1 + j\omega \tau_e}$$

$$= \frac{C_1}{R_1} \cdot \frac{1}{1 + j\omega(\tau_c + \tau_e)}$$

The log-log plot of this function is shown in Fig. A.3. and may be compared with the experimental results of Fig. II.6.

Appendix B

Circuit Details

Brief notes together with circuit diagrams of those electronic items not previously given in detail in the text are appended below.

1. 400c/s. Generator.
2. Generator Field Power Amplifier.
3. Ripple Filter Power Amplifier.
4. Narrow Band Amplifier.
5. D.C. Amplifier.
6. Modulation Supply.

(In addition to the above list, other items which constructed but later discarded (Sect.III) include a narrow band amplifier selective to 12.5c/s a phase shifter and a wide band amplifier with lower frequency limit 0.1 c/s.)

400 c/s. Generator

The Wien Bridge Oscillator of fig.B1 is freely tuned to 400 c/s. and is then locked to the 50 c/s. mains frequency by a synchronising signal which is obtained by filtering out the fourth harmonic from the rectifier ripple by means of the tuned primary, tuned secondary, transformer T_1.

In the following power stage, the outputs are taken from the transformer T_2. Two identical secondary windings provide equal reference signals for the phase sensitive rectifier, while a third winding provides a signal which, after passing through a 0 - 180 phase shifter, is used to provide the modulation (either field or frequency) for the Transitron N.M.R. field discriminator

(The author is indebted to Mr.E.Laisk of the Electronic Workshop for the design of this circuit.)

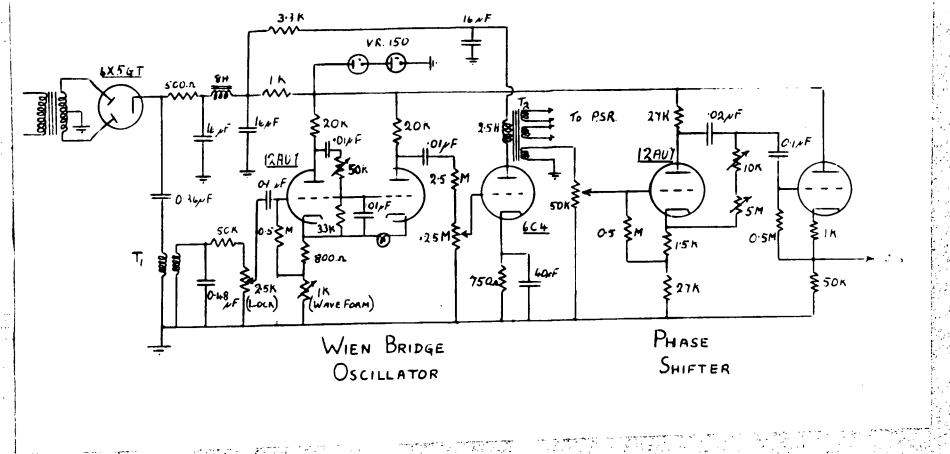

FIG B·1

Generator Field Power Amplifier

The generator field coils form the plate load of four 6AS7 twin-triodes which are connected in parallel. The plate supply of 180 volts is obtained from a bank of storage cells, and the tubes are capable of delivering a maximum plate current of 1 amp..

The 6J6 twin-triode acts as a pre-amplifier and provides for two separate inputs. The H.T. power supply is not directly earthed and the output is taken from a potentiometer across the H.T. thus allowing the correct bias to be applied to the grids of the power tubes.

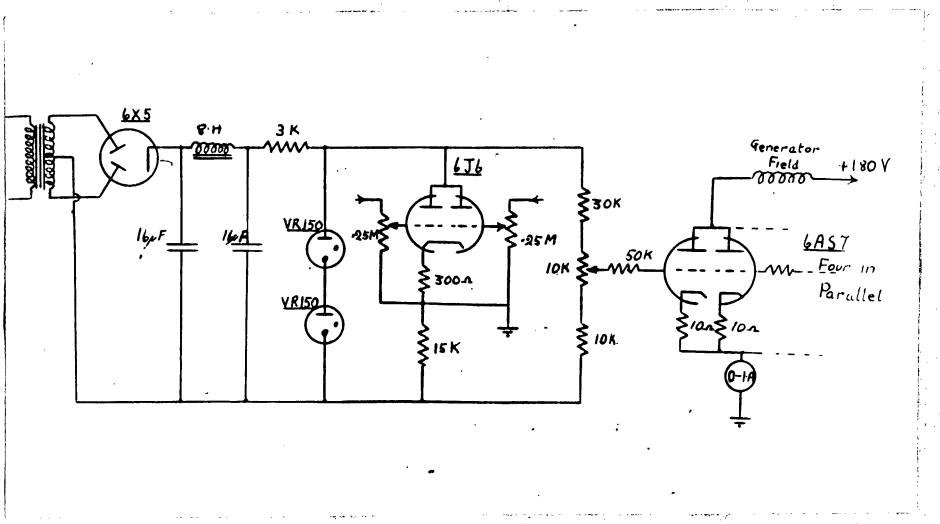

Fig B·2

RippleFilter Power Amplifier

The bank of four 6AS7 power tubes are connected in parallel across the magnet terminals, the d.c. voltage of which provides the necessary plate supply. The ripple voltage existing at the magnet terminals is amplified by the 12AX7 cascode amplifier with 12AU7 cathode follower output.

The subsequent 6J6 stage produces little further gain but is designed to provide the necessary phase inversal and correct negative bias for the power tubes. The filter in the input circuit prevents the occurance of self-oscillation.

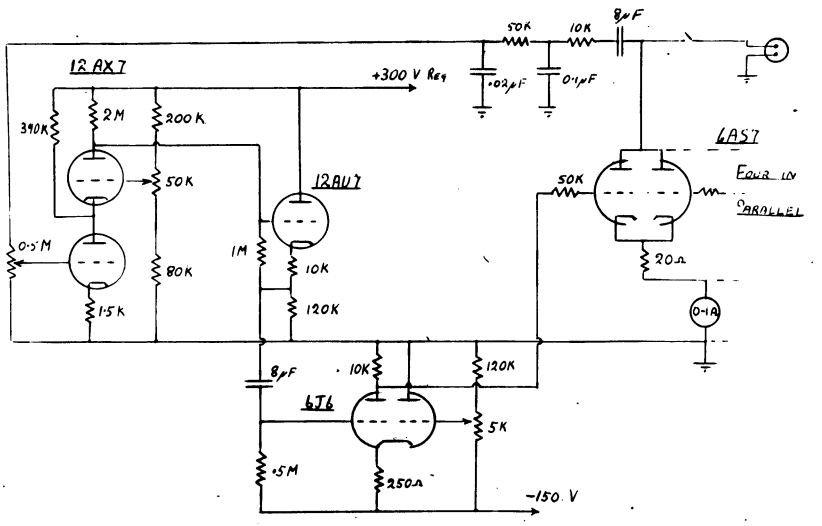

Fig B·3

Narrow Band Amplifier

The first stage of amplification has a cathode follower output in order to provide the necessary low impedance cathode coupling to the second stage. Negative feedback is introduced in the second stage by means of the twin-T network which rejects the frequency to which it is tuned(in this case 400 c/s.). At this frequency therefore the maximum stage gain is obtained; while at other frequencies the stage gain is reduced by the negative feedback. The theoretical Q of this stage is $\frac{A+1}{4}$ where A is the stage gain. By closing the switch S the negative feedback is shorted out and wide band amplification is obtained.

(Erratum: the 6V6 of the output stage is triode connected and the diagram should show the screen grid connected to the plate.)

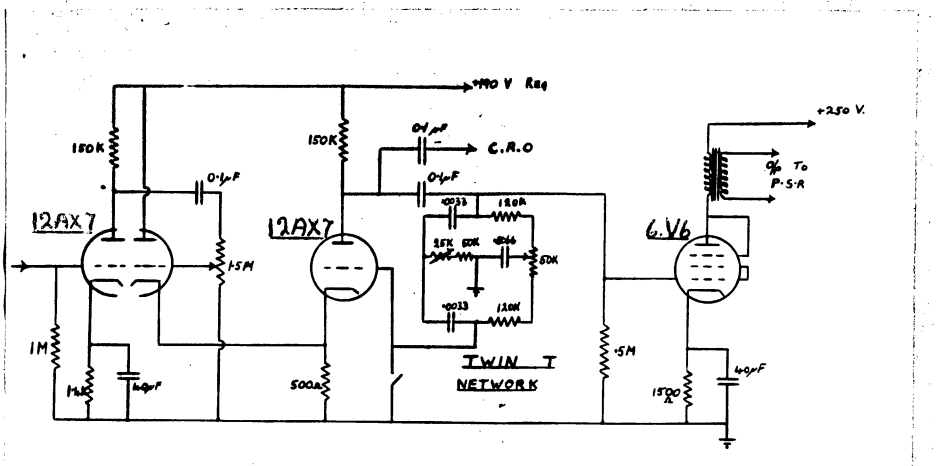

NARROW-BAND AMPLIFIER

Fig B·4

D.C. Amplifier

In the first stage of the d.c. amplifier, the 6J6 twin-triode employs cathode follower compensation against cathode drift. The output is taken from between the load resistor and a potentiometer placed across the H.T. By adjustment of the pot. the correct working point for the 12AX7 of the second stage is obtained. It also enables the floating power supply of the second stage to be indirectly connected to earth.

By employing a cathode load in the second stage and by taking the output from a pot. across the H.T., it is possible to ensure that the output is at earth potential, thus facilitating the connection of subsequent equipment.

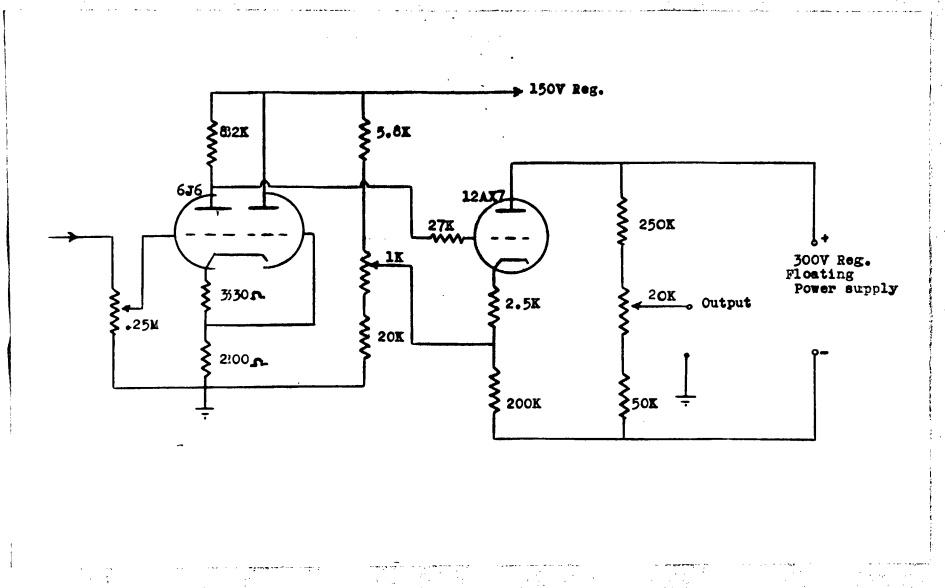

Fig B·5

Modulation Supply

In order to obtain the necessary drive, the field modulation coils or the frequency "wobbulator" (depending upon whether field or frequency modulation is required) is connected directly into the cathode circuit of the two parallel, triode-connected 6V6 tubes. This power stage is preceded by the 12AU7 voltage pre-amplification stage to which the modulation signal from the 400c/s. generator is applied.

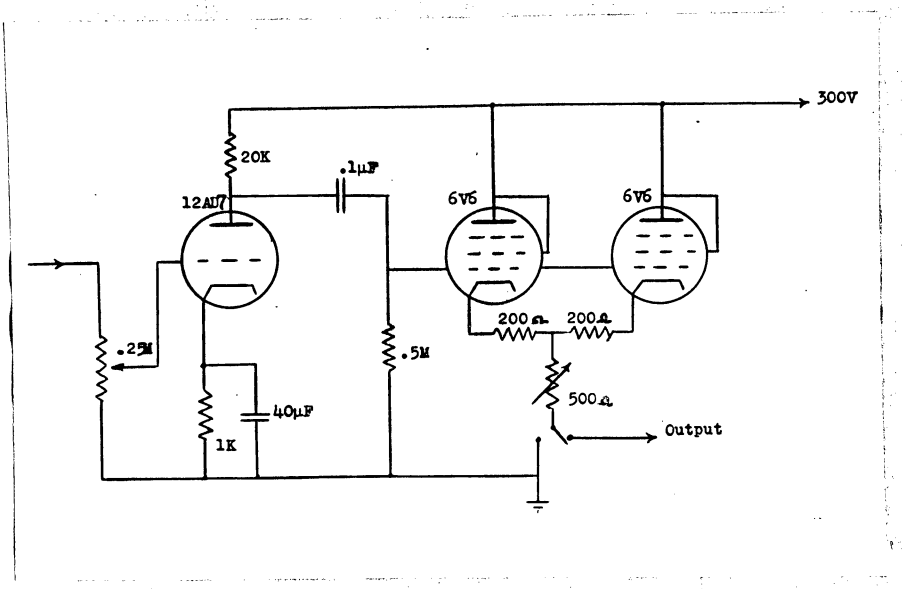

FIG B·6